The Heston Model with Term Structure

Master's Thesis
by
Jiayuan Li

Supervisors:
Prof. Dr. Ir. C.W. Oosterlee
Dr. Bert-Jan Nauta
Dr. Vitaly Braude

Other Thesis Committee Members:
Dr. Ir. J.A.M. Van Der Weide
Dr. Ir. Fred Vermolen

Faculty of Electrical Engineering, Mathematics and
Computer Science
Institute of Applied Mathematics

June 18, 2009

Acknowledgments

There are many people that I would like to thank, in particular Kees Oosterlee, who not only serves as my supervisor during the past two years, but also encourages and challenges me throughout the period of my thesis project. The same thanks should also go to my supervisor Bert-jan Nauta and daily supervisor Vitaly Braude in ABN AMRO, who take great efforts in guiding me through the whole internship period. I would also like to thank Tim Mexner and Vincent Leijdekker in our team, who offer me much help in understanding the related financial concepts and programming details, and Neeltje van de Wiel, Stanislav Zakovic and Reinhardt Chamonal, who provide me with their IT support. I am also very grateful to Fang Fang for the fruitful discussion with her and to Alberto Elices and Thomas Lidebrandt for kindly answering my questions about their papers. Furthermore, I want to thank the other committe members; Hans van der Weide and Fred Vermolen. Last but not least, great love goes out to my parents who have supported me and gratitude to all of my friends who have helped me. In brief, without the help of these persons, this Masters Thesis would not be a success. Thank you all.

Abstract

The purpose of this project is to extend the Heston model in order to incorporate the term structure (TS) of the implied volatility surface. This includes implementing a TS within the Heston model and its calibration to a set of market instruments. The TS Heston model with piecewise constant parameters is implemented to match the TS and the COS pricing method is used for fast option pricing. We calibrate the model to the EUR/USD and USD/JPY market data and historic data is also used to test the robustness of the model. Then the model with calibrated parameters are used to price exotic options by means of Monte Carlo simulation with a new control variate we propose. Finally we also propose the COS method for pricing discrete barrier options as future research directions.

Contents

1 Introduction

1.1 Options and their pricing

It was not until the publication of the Black-Scholes model in 1973 that the era of using mathematical models to price options and hedge risks started.

An option is a contract between a buyer and a seller that gives the buyer the right, but not the obligation, to buy or to sell a particular asset (the underlying asset) at a later day (at or before the maturity) at an agreed price (the strike price). In return for granting the option, the seller charges a premium from the buyer. A call option gives the buyer the right to buy the underlying asset; a put option gives the buyer of the option the right to sell the underlying asset. If the buyer chooses to exercise this right, the seller is obliged to sell or buy the asset at the agreed price; otherwise the option just expires after the maturity.

Investors buy options either as speculators or as hedgers. As speculators, they bet on the upward movement of the underlying asset by buying a call option, or on the downward movement of the underlying asset by buying a put option. As hedgers, they either want to buy or sell certain underlying asset in the future, and by buying the corresponding options, they either fix the maximum price they need to pay if they want to buy, or lock the maximum loss they will suffer if they want to sell; or they want to hedge the risks for the underlying asset they own or owe by trading options whose value move in the opposite direction of the underlying asset.

There are mainly two types of options, exchange-traded options and over-the-counter options. Exchange-traded options form an important class of options which have standardized contract features and are traded on public exchanges, facilitating trading among independent parties. They include stock options, commodity options, bond options, stock market index options and options on futures contracts. Over-the-counter options are traded between private parties, often well-capitalized institutions that have negotiated separate trading and clearing arrangements with each other. They include interest rate options, equity options and foreign exchange (FX) options. In this thesis, we focus on the FX options, although we expect the results can be extended to equity options as well.

When traders trade options, the need to know their prices. Hence, the valuation of options become very important and their values can be estimated using a variety of quantitative techniques based on the concept of risk neutral pricing and using stochastic calculus. The first and most basic model is the Black-Scholes model. More sophisticated models are those which also incorporate the volatility smile, a pattern in which at-the-money options tend to have lower implied volatilities than in- or out-of-the-money options.

A model usually has several parameters which need to be predefined. Some of them are quite obvious, such as the interest rate. Others are more tricky and in order to make the model consistent with the current market situation, we get their values by calibrating the model to the market data, usually the most liquid exchange-traded options.

In the calibration process, we first set initial values to the model parameters and then

search for the best set of parameters which minimize the differences between the model outputs and the market data. If a set of parameters which reproduces the market data within a reasonable accuracy can be found, then the calibration is successful and we can use the model to price the exotic options.

In some models, analytic solutions exist for certain options. Then they can be priced fast and accurately. For others, Monte Carlo simulation is often used. A number of random price paths of the underlying asset are generated, each of which results in a payoff for the option. Then these payoffs are averaged and discounted to yield an expectation value for the option.

1.2 Project description

In the Black-Scholes model, constant volatility throughout all the strikes and maturities is assumed. This was indeed the case in the market at that time until the market crash in 1987, after which people started to observe the volatility smile. Hence, researchers have proposed various extensions of the Black-Scholes model for pricing options that aim to incorporate the market observed implied volatility smile. The two most popular ones that are used for path-dependent options are the local volatility model and the Heston stochastic volatility model [1].

Dupire has shown [24] that the local volatility model can exactly reproduce the prices of all vanilla call/puts at a continuous range of strikes and maturities. Given this range the local volatility model is completely determined. One disadvantage of the model is that it has only one stochastic factor and the volatility is a deterministic function of the spot price and time. However, it is clear for many markets that the correlation between spot and implied volatility is not close to 1. Therefore the model is not fully realistic which may affect pricing of some path-dependent options significantly.

In the Heston stochastic volatility model, the volatility follows a stochastic and mean-reverting process. It has this extra stochastic factor which makes the model more realistic. Its popularity among practitioners comes from the fact that it has semi-analytical expressions for prices of vanillas, which makes fast and accurate calibration possible. This calibration assumes time-independent parameters. In practice one often calibrates to the smile observed at one maturity, thus accepting that the model will not reproduce the prices of all vanillas.

However, besides the above calibration issue, the assumption of constant parameters provides an issue for risk managing a book of multiple path-dependent options. Assume the model calibrates to the maturity of the option. Then a book with multiple options with different maturities, that are all valued and risk managed on Heston, is actually not handled by the same model, because the Heston parameters for each model may be different. To stress the point, it may be that the instantaneous volatility at time zero varies significantly over different calibrated models (implying they disagree on the current level of instantaneous volatility).

In this project, we compare different ways of incorporating the term structure into the Heston model and implement the model with piecewise constant parameters. In the calibra-

tion process, we employ a recently proposed pricing method called the COS method. The combination of these two produce fast and accurate results for the calibration of certain market data. Then we use the calibrated model to price some exotic options using Monte Carlo simulation. Here, we propose a new control variate to reduce the variance. We also propose to apply COS method to price discrete barrier options as a future research direction.

The thesis is organized in ten sections. Section 2 introduces the market conventions in the FX market. Section 3 presents the derivation of the characteristic function of the TS Heston model with piecewise constant parameters. Section 4 presents the COS pricing method for the European-style options. Section 5 discusses the details of calibration. Section 6 applies the calibration method to calibrate the EUR/USD and USD/JPY market data. Section 7 does some jump tests to see whether jumps exist or not in the historic market data and calibrate our model to them. Section 8 proposes a new control variate for variance reduction in Monte Carlo simulation for pricing exotic options and shows the simulation results and the variance reduction achieved. Section 9 discusses the possibility of applying COS method on discrete barrier options as a future research direction. Section 10 concludes the thesis.

2 FX market

In the FX market, the European options are quoted in implied volatilities rather than in option prices directly [2]. Furthermore, those implied volatilities are quoted in terms of delta rather than strike. Given the implied volatility and delta, we can easily calculate the strike and further the option price using the Black-Scholes equation.

Usually for each maturity, five quotes are available in the market: At-The-Money Straddle (ATM), 25-Δ Risk Reversal (RR), 25-Δ Strangle (STR), 10-Δ Risk Reversal and 10-Δ Strangle. The last two are not so liquid since they are far out-of-the-money. Therefore, we will only use the market data of the first three in the calibration.

2.1 Delta conventions

The FX market employs quite complicated delta conventions for different currency pairs and different maturities, namely (spot) delta and forward delta, delta including the premium and delta excluding the premium.

The value of a vanilla option in the Black-Scholes model is calculated as follows:

$$C_0 = \alpha \left(e^{-r_f T_d} S_0 N(\alpha d_1) - e^{-r_d T_d} K N(\alpha d_2) \right) \tag{1}$$

where

$$d_1 = \frac{\log(S_0/K) + (r_d - r_f)T_d + v^2 T_e/2}{v\sqrt{T_e}} \text{ and } d_2 = d_1 - v\sqrt{T_e} \tag{2}$$

Here α is put-call type with $\alpha = 1$ for a call and $\alpha = -1$ for a put, T_d is time from spot until the delivery date, T_e is time from today until the expiry date, $r_{d/f}$ is continuously compounded zero rate for the domestic/foreign currency corresponding to the delivery date of the option, K is the strike of the option, v is the volatility, S_0 is the initial FX spot and $N(\cdot)$ is the standard normal distribution function.

The (spot) delta of the option is

$$\Delta_{BS} = \frac{\partial C_0}{\partial S_0} = \alpha e^{-r_f T_d} N(\alpha d_1) \tag{3}$$

In all the markets except the EUR/USD market, the premium (C_0) is included in the delta. This delta is called the "left-side delta" and is defined as:

$$\Delta_L = \Delta_{BS} - \frac{C_0}{S_0} = \alpha \cdot \frac{K}{S_0} e^{-r_d T_d} N(\alpha d_2) \tag{4}$$

The logic of the left-side delta is as follows: Consider a bank that sells a call on the foreign currency and needs to do delta hedging in that currency. The amount that the bank has to buy is $\Delta_{BS} S_0 - C_0$ since it receives the premium in foreign currency. This is how Δ_L is defined in equation (4).

For emerging markets (EM) and for maturities of more than two years (including 2 years), it is usual for forward delta's to be quoted (it is called driftless delta in [7]). They are defined as follows:

$$\Delta_{BS}^{F} = e^{r_f T_d}\Delta_{BS} \text{ and } \Delta_{L}^{F} = e^{r_f T_d}\Delta_{L} \tag{5}$$

2.2 ATM straddle, 25-Δ risk reversal and 25-Δ strangle

By convention the implied volatilities are quoted in terms of the ATM Straddle, 25-Δ RR and 25-Δ STR.

The ATM is a zero delta straddle consisting of both a call option and a put option, with the same expiry T and with the same strike price. The strike price is chosen in such way that the delta of the straddle is equal to zero, i.e. the call delta is equal to the opposite of the put delta. Hence, for the EUR/USD market, we have $N(d_1) = \frac{1}{2}$ according to equations (3) and (5). For other markets, we have $N(d_2) = \frac{1}{2}$ according to equations (4) and (5). Thus, the ATM strike can be calculated analytically. The table below shows the ATM delta and the ATM strike.

	ATM Delta	ATM Strike	Market
Δ_{BS}	$\alpha e^{-r_f T_d}/2$	$S_0 e^{(r_d - r_f)T_d + v_{ATM}^2 T_e/2}$	EUR/USD maturities$\leq$ 1y
Δ_{BS}^{F}	$\alpha/2$	$S_0 e^{(r_d - r_f)T_d + v_{ATM}^2 T_e/2}$	EUR/USD maturities$>$ 1y
Δ_{L}	$\alpha e^{-r_f T_d - v_{ATM}^2 T_e/2}/2$	$S_0 e^{(r_d - r_f)T_d - v_{ATM}^2 T_e/2}$	maturities$\leq$ 1y
Δ_{L}^{F}	$\alpha e^{-v_{ATM}^2 T_e/2}/2$	$S_0 e^{(r_d - r_f)T_d - v_{ATM}^2 T_e/2}$	maturities$>$ 1y, EM

Table 1: ATM Delta and strike for different delta definitions [2]

A 25-Δ RR is a portfolio consisting of a long 25-Δ call and a short 25-Δ put with the same expiry. A 25-Δ RR quote is hence the difference between the volatility of a 25-Δ call and a 25-Δ put.

A 25-Δ STR is a portfolio consisting of long both a 25-Δ call and a 25-Δ put option with the same expiry. A 25-Δ STR quote is equal to the average volatility of a 25-Δ call and a 25-Δ put minus the ATM volatility.

Therefore, the volatility of a 25-delta call and put can be obtained from these quotes as follows

$$v_{C,25} = v_{ATM} + STR_{25} + \frac{1}{2}RR_{25} \tag{6}$$

$$v_{P,25} = v_{ATM} + STR_{25} - \frac{1}{2}RR_{25} \tag{7}$$

3 Heston model and TS Heston model

In finance, the Heston model, named after Steven Heston, is a mathematical model describing the evolution of the volatility of an underlying asset. It is a stochastic volatility model: such a model assumes that the volatility of the asset is not constant, nor even deterministic, but follows a random process [21].

In (ordinary) Heston model, all the parameters (normally five) are time-independent. Hence, the model can be calibrated to at most four market instruments. Since we want to calibrate to more than four market instruments with different maturities, we try to make them piecewise constant and thus get the TS Heston model.

3.1 Heston's stochastic volatility model

Let $S(t)$ be the FX spot at time t, r_d and r_f be the domestic and foreign short rates. Then we assume that $S(t)$ is governed by the following SDEs in (risk-neutral) pricing measure:

$$\begin{aligned} \mathrm{d}S &= (r_d - r_f)S\mathrm{d}t + \sqrt{v}S\mathrm{d}W_1, \\ \mathrm{d}v &= \kappa(\theta - v)\mathrm{d}t + \sigma\sqrt{v}\mathrm{d}W_2, \\ \mathrm{Cov}[\mathrm{d}W_1, \mathrm{d}W_2] &= \rho\,\mathrm{d}t \end{aligned} \tag{8}$$

where κ, σ and θ are the mean reversion rate, the volatility of the variance and the mean reversion level.

Define $x = \log(S)$ and $\mu = r_d - r_f$. We then have

$$\begin{aligned} \mathrm{d}x &= (\mu - \frac{1}{2}v)\mathrm{d}t + \sqrt{v}\mathrm{d}W_1, \\ \mathrm{d}v &= \kappa(\theta - v)\mathrm{d}t + \sigma\sqrt{v}\mathrm{d}W_2 \end{aligned} \tag{9}$$

The joint characteristic function on the interval $[0, T]$ is defined as follows:

$$\phi_{0T}(X, V|x_0, v_0) = E(e^{iXx_T + iVv_T}|x_0, v_0) \tag{10}$$

and the marginal characteristic function for the logarithm of the underlying asset on the same interval is defined as:

$$\phi_{0T}(X|x_0, v_0) = E(e^{iXx_T}|x_0, v_0) = \phi_{0T}(X, V|x_0, v_0)|_{V=0} \tag{11}$$

The analytic formula of the marginal characteristic function is given by Heston in [25]. Elices [4] derives an analytic formula for the joint characteristic function where the marginal characteristic function of the log-asset price can be obtained by evaluating the joint characteristic function at V = 0:

$$\phi_{0T}(X, V|x_0, v_0) = \exp(C(X, V) + D(X, V)v_0 + iXx_0) \tag{12}$$

Here (X, V) is in the dual space of (x, v). The coefficients of the characteristic function are given by

$$\begin{cases} C(X,V) = i\mu X\tau + \frac{\kappa\theta}{\sigma^2}\left(\log\left(\frac{1-\tilde{g}e^{-d\tau}}{1-\tilde{g}}\right)^{-2} + (\kappa - i\rho\sigma X - d)\tau\right) + C^0 \\ D(X,V) = \frac{\kappa - i\rho\sigma X - d}{\sigma^2}\left(\frac{g-\tilde{g}e^{-d\tau}}{1-\tilde{g}e^{-d\tau}}\right) \end{cases} \tag{13}$$

where $\tilde{g} = \frac{\kappa - i\rho\sigma X - d - D^0\sigma^2}{\kappa - i\rho\sigma X + d - D^0\sigma^2}$, $g = \frac{\kappa - i\rho\sigma X - d}{\kappa - i\rho\sigma X + d}$, $d = \sqrt{(\kappa - i\rho\sigma X)^2 + \sigma^2 X(i + X)}$, $C^0 = 0$, $D^0 = iV$ and the length of the period $\tau = T$.

Because of its analytic feature, the prices of the European options can be calculated much more easily using Fourier inversion techniques for example. Hence, the Heston model is widely used by practioners.

3.2 Characteristic function of TS Heston model with piecewise constant parameters

Despite its popularity, the Heston model also has its own limitations. Since the coefficients of the characteristic function are solutions of ordinary differential equations of Riccati type, most of the parameters cannot be time-dependent if we want the coefficients to be analytic. This however causes a problem if we want to calibrate to options of different maturities. For each maturity, we may get completely different sets of parameters, and what is more, the initial variance may disagree as well.

To solve this problem, we incorporate the term structure information. To achieve that, the Heston model has to be generalized in order to allow for time dependence in its coefficients [8]. Time dependence is most easily added to the mean-reversion level θ, since this parameter does not enter in the non-linear Ricatti equation. Hence the solution can be constructed for arbitrary $\theta(t)$ by means of numerical calculation of integrals over time. For the other Heston model parameters, the generalization to the time-dependent model is not so straightforward. Some analytic solutions are possible for specific choices of the time dependence, but in general the solution can only be found by numerical integration of the two-dimensional system of differential equations. Since we will not be able to get analytic solutions of the characteristic functions in general, these methods are not in our favor.

As an alternative, Mikhailov [8] et al proposed the idea of using piecewise constant parameters. The parameters are kept constant in one time interval, but different for other intervals. The coefficients of the characteristic function are derived by solving the differential equations from the last period till the first period, where the solution of the past period is used as initial condition for the preceding one. Elices [4], however, derives the characteristic functions in a different way. He proposes the way of deriving the characteristic function of two consecutive periods from the characteristic functions of each period. Due to its recursive feature, we hence adopt his way to derive the characteristic functions of models with piecewise constant parameters.

According to [4], we consider an N-dimensional Markov process $\mathbf{x}(t) = (x_1(t), ..., x_N(t))$ and the family of exponential characteristic functions of the form (14) with exponents linear in the stochastic processes $\mathbf{x}_u$ at time t_u in the time interval from t_u to t_v. (The Heston process, as we have shown, consists of (x_0, v_0) and also has the same form of characteristic function.) The characteristic function thus reads:

$$\phi_{uv}(\mathbf{X}|\mathbf{x}_u) = \exp(C_{uv}(\mathbf{X}) + \mathbf{D}_{uv}(\mathbf{X}) \cdot \mathbf{x}_u) \tag{14}$$

Here, $\mathbf{X} = (X_1(t), ..., X_N(t))$ is in the dual space of $\mathbf{x}(t)$ and $\mathbf{D}_{uv}(\mathbf{X}) \cdot \mathbf{x}_u = \sum_{i=1}^{N} D_{uv,i}(\mathbf{X}) x_i(t_u)$ refers to the inner product.

The criterion of the linearity of exponents is actually very important. We will show that if a process has different characteristic functions in different time intervals but all with linear exponents, the characteristic function in the overall time interval still has that property.

Now suppose $\phi_{0u}(\mathbf{X}|\mathbf{x}_0)$ describes the process from 0 to t_u and $\phi_{uv}(\mathbf{X}|\mathbf{x}_u)$ describes the process from t_u to t_v. We want to obtain $\phi_{0v}(\mathbf{X}|\mathbf{x}_0)$ in terms of $\phi_{0u}(\mathbf{X}|\mathbf{x}_0)$ and $\phi_{uv}(\mathbf{X}|\mathbf{x}_u)$.

The definition of the characteristic function is as follows:

$$\phi_{0v}(\mathbf{X}|\mathbf{x}_0) = \int_{\mathbf{R}^N} e^{i\mathbf{X}\cdot\mathbf{x}_v} f_{0v}(\mathbf{x}_v|\mathbf{x}_0) d\mathbf{x}_v \tag{15}$$

As the process is Markov, the time interval $[0, t_u]$ is independent from $[t_u, t_v]$. Hence, the density function can be written as

$$f_{0v}(\mathbf{x}_v|\mathbf{x}_0) = \int_{\mathbf{R}^N} f_{uv}(\mathbf{x}_v|\mathbf{x}_u) f_{0u}(\mathbf{x}_u|\mathbf{x}_0) d\mathbf{x}_u \tag{16}$$

Substituting equation (16) into (15) and exchanging the integration order yields:

$$\begin{aligned}\phi_{0v}(\mathbf{X}|\mathbf{x}_0) &= \int_{\mathbf{R}^N} f_{0u}(\mathbf{x}_u|\mathbf{x}_0) \int_{\mathbf{R}^N} e^{i\mathbf{X}\cdot\mathbf{x}_v} f_{uv}(\mathbf{x}_v|\mathbf{x}_u) d\mathbf{x}_v d\mathbf{x}_u \\ &= \int_{\mathbf{R}^N} f_{0u}(\mathbf{x}_u|\mathbf{x}_0) \phi_{uv}(\mathbf{X}|\mathbf{x}_u) d\mathbf{x}_u \end{aligned} \tag{17}$$

Substituting equation (14) into (17) yields:

$$\begin{aligned}\phi_{0v}(\mathbf{X}|\mathbf{x}_0) &= \int_{\mathbf{R}^N} f_{0u}(\mathbf{x}_u|\mathbf{x}_0) \exp(C_{uv}(\mathbf{X}) + \mathbf{D}_{uv}(\mathbf{X}) \cdot \mathbf{x}_u) d\mathbf{x}_u \\ &= \exp(C_{uv}(\mathbf{X})) \int_{\mathbf{R}^N} f_{0u}(\mathbf{x}_u|\mathbf{x}_0) \exp(i \cdot (i^{-1}\mathbf{D}_{uv}(\mathbf{X})) \cdot \mathbf{x}_u) d\mathbf{x}_u \\ &= \exp(C_{uv}(\mathbf{X})) \phi_{0u}(i^{-1}\mathbf{D}_{uv}(\mathbf{X})|\mathbf{x}_0) \\ &= \exp(C_{uv}(\mathbf{X}) + C_{0u}(i^{-1}\mathbf{D}_{uv}(\mathbf{X})) + \mathbf{D}_{0u}(i^{-1}\mathbf{D}_{uv}(\mathbf{X})) \cdot \mathbf{x}_0) \end{aligned} \tag{18}$$

Hence, $\phi_{0v}(\mathbf{X}|\mathbf{x}_0)$ still belongs to the family of exponential characteristic functions with linear exponents. Applying equation (14) to the time interval $[0, t_v]$ yields:

$$\phi_{0v}(\mathbf{X}|\mathbf{x}_0) = \exp(C_{0v}(\mathbf{X}) + \mathbf{D}_{0v}(\mathbf{X}) \cdot \mathbf{x}_0) \tag{19}$$

Equating the coefficients of equation (18) and equation (19) yields:

$$\begin{cases} C_{0v}(\mathbf{X}) = C_{uv}(\mathbf{X}) + C_{0u}(i^{-1}\mathbf{D}_{uv}(\mathbf{X})) \\ \mathbf{D}_{0v}(\mathbf{X}) = \mathbf{D}_{0u}(i^{-1}\mathbf{D}_{uv}(\mathbf{X})) \end{cases} \tag{20}$$

Applying this procedure, we obtain the characteristic function of any consecutive periods.

We can also get the recursion formula by applying the principle of iterated expectations. According to equation (11), the characteristic function $\phi_{uv}(\mathbf{X}|\mathbf{x}_u)$ for any time interval $[t_u, t_v]$ is given by

$$\phi_{uv}(\mathbf{X}|\mathbf{x}_u) = E(e^{i\mathbf{X}\cdot\mathbf{x}_v}|\mathbf{x}_u) \tag{21}$$

Suppose $\phi_{uv}(\mathbf{X}|\mathbf{x}_u)$ also satisfies equation (14). Considering the time interval $[0, t_v]$ and using the iterated expectations, we have

$$\begin{aligned} \phi_{0v}(\mathbf{X}|\mathbf{x}_0) &= E(e^{i\mathbf{X}\cdot\mathbf{x}_v}|\mathbf{x}_0) \\ &= E(E(e^{i\mathbf{X}\cdot\mathbf{x}_v}|\mathbf{x}_u)|\mathbf{x}_0) \\ &= E(\phi_{uv}(\mathbf{X}|\mathbf{x}_u)|\mathbf{x}_0) \\ &= E(e^{C_{uv}(\mathbf{X})+\mathbf{D}_{uv}(\mathbf{X})\cdot\mathbf{x}_u}|\mathbf{x}_0) \\ &= \exp(C_{uv}(\mathbf{X}))E(\exp(\mathbf{D}_{uv}(\mathbf{X})\cdot\mathbf{x}_u)|\mathbf{x}_0) \\ &= \exp(C_{uv}(\mathbf{X}))E(\exp(i\cdot i^{-1}\mathbf{D}_{uv}(\mathbf{X})\cdot\mathbf{x}_u)|\mathbf{x}_0) \\ &= \exp(C_{uv}(\mathbf{X}))\phi_{0u}(i^{-1}\mathbf{D}_{uv}(\mathbf{X})|\mathbf{x}_0) \\ &= \exp(C_{uv}(\mathbf{X}) + C_{0u}(i^{-1}\mathbf{D}_{uv}(\mathbf{X})) + \mathbf{D}_{0u}(i^{-1}\mathbf{D}_{uv}(\mathbf{X}))\cdot\mathbf{x}_0) \end{aligned} \tag{22}$$

which is the same as equation (18).

For the Heston model with constant parameters in the interval $[t_u, t_v]$, according to (12), the characteristic function reads:

$$\phi_{uv}(\mathbf{X}|\mathbf{x}_u) = \exp(C_{uv}(\mathbf{X}) + D_{uv,2}(\mathbf{X})v(t_u) + D_{uv,1}(\mathbf{X})x(t_u)) \tag{23}$$

where $\mathbf{X} = (X, V)$, $\mathbf{x_u} = (x(t_u), v(t_u))$, $D_{uv,1}(X, V) = iX$ and $C_{uv}(X, V)$ and $D_{uv,2}(X, V)$ are given by equations (13) ($D_{uv,2}(X, V) = D(X, V)$).

Suppose we already have the characteristic function of the interval $[0, t_u]$, we obtain the coefficients in (19) using recursive equation (20):

$$\begin{cases} C_{0v}(X, V) = C_{uv}(X, V) + C_{0u}(X, i^{-1}D_{uv,2}(X, V)) \\ D_{0v,2}(X, V) = D_{0u}(X, i^{-1}D_{uv,2}(X, V)) \\ D_{0v,1}(X, V) = iX \end{cases} \tag{24}$$

If we continue with the recursive procedure, the joint characteristic function from 0 to any time can be derived, and the marginal characteristic function of the log-asset price can be obtained according to (11) for pricing European options.

What is worth mentioning here is that as one can see from equation (13), the characteristic function of the Heston model contains a complex logarithm, which is a multivalued function.

According to the literature [28], one should be careful in choosing the correct branch. If we restrict the logarithm to its principal branch, the characteristic function may become discontinuous, leading to completely wrong option prices if options are priced by Fourier inversion. Kahl and Jäckel [29] propose the phase rotation count technique to solve this problem. However, in a later paper, Lord and Kahl [5] proved that for Heston-like models, we can restrict the logarithm to its principal branch, and the resulting characteristic function is the correct one for all complex ω in the strip of analycity of the characteristic function. Therefore, in our implementation, we just choose the principal branch.

4 COS pricing method

The calibration process involves a very large number of option price evaluations with many different parameter settings. Hence efficient numerical methods are required to rapidly price the options.

Existing numerical methods can be classified into three categories: partial-(integro) differential equation methods, Monte Carlo simulation and numerical integration methods. When characteristic functions are known analytically, the integration methods are always used for calibration purposes. State-of-the-art numerical integration techniques have in common that they all rely on a transformation to the Fourier domain, among which the Carr-Madan method [6] is most widely used. Instead of using FFT, Fang and Oosterlee [3] recently proposed a new method, called COS method, which is based on Fourier-cosine expansions. The COS method is found to be superior to the Carr-Madan and other methods with respect to both speed and accuracy for among others the Heston model. We extend its use to the term structure Heston model in this paper.

4.1 COS pricing method

In this section, we summarize the COS pricing method for the European-style options proposed in [3].

The point-of-departure for pricing European options with numerical integration techniques is the risk-neutral valuation formula:

$$C(x,t_0) = e^{-r\Delta t}E^{\mathbb{Q}}[C(y,T)|x] = e^{-r\Delta t}\int_{\mathbb{R}} C(y,T)f(y|x)dy \tag{25}$$

where C denotes the option value, Δt is the difference between the maturity T and the initial date t_0, $E^{\mathbb{Q}}[\cdot]$ is the expectation operator under risk-neutral measure $\mathbb{Q}$, x and y are state variables at time t_0 and T respectively, and $f(y|x)$ is the probability density of y given x, and r is the risk-neutral interest rate.

The probability density function which appears in the integration of the pricing formula is not known for many relevant pricing processes. However, its Fourier transform, the characteristic function, is often available. Hence, the main idea here is to reconstruct the whole integral from its Fourier-cosine series expansion (also called 'cosine expansion') where the characteristic function rather than the density function is involved, since Fourier-cosine series expansions usually give an optimal approximation of functions with a finite support.

For functions supported on a finite interval, say $[a,b] \subset \mathbb{R}$, the Fourier-cosine series expansion reads

$$f(x) = \sum_{k=0}^{\infty}{}' A_k \cdot \cos(k\pi\frac{x-a}{b-a}) \tag{26}$$

with

$$A_k = \frac{2}{b-a}\int_a^b f(x)\cos(k\pi\frac{x-a}{b-a})dx \tag{27}$$

Here $\sum'$ indicates that the first term in the summation is weighted by one-half.

Suppose $[a,b] \subset \mathbb{R}$ is chosen such that the truncated integral approximates the infinite counterpart very well, i.e.

$$\phi_1(\omega) := \int_a^b e^{i\omega x} f(x)dx \approx \int_{\mathbb{R}} e^{i\omega x} f(x)dx = \phi(\omega) \tag{28}$$

Thus,

$$A_k = \frac{2}{b-a} Re\left\{\phi_1\left(\frac{k\pi}{b-a}\right) \cdot \exp\left(-i\frac{ka\pi}{b-a}\right)\right\} \tag{29}$$

and $A_k \approx F_k$ with

$$F_k = \frac{2}{b-a} Re\left\{\phi\left(\frac{k\pi}{b-a}\right) \cdot \exp\left(-i\frac{ka\pi}{b-a}\right)\right\} \tag{30}$$

We now replace A_k by F_k in the series expansion of $f(x)$ on $[a,b]$, i.e.

$$f_1(x) = \sum_{k=0}^{\infty}{}' F_k \cdot \cos(k\pi\frac{x-a}{b-a}) \tag{31}$$

and truncate the series summation such that

$$f_2(x) = \sum_{k=0}^{N-1}{}' F_k \cdot \cos(k\pi\frac{x-a}{b-a}) \tag{32}$$

Now we derive the COS formula for European-style options by replacing the density function by its Fourier-cosine series. Since the density rapidly decays to zero as $y \to \pm\infty$ in equation (25), we truncate the infinite integration range to $[a,b] \subset R$ without losing significant accuracy, and we obtain approximation C_1:

$$C_1(x,t_0) = e^{-r\Delta t} \int_a^b C(y,T) f(y|x) dy \tag{33}$$

Since $f(y|x)$ is usually not known whereas the characteristic function is, we replace the density by its cosine expansion in y,

$$f(y|x) = \sum_{k=0}^{\infty}{}' A_k(x) \cdot \cos(k\pi\frac{y-a}{b-a}) \tag{34}$$

with

$$A_k(x) = \frac{2}{b-a} \int_a^b f(y|x) \cos(k\pi\frac{y-a}{b-a}) dy \tag{35}$$

so that

$$C_1(x,t_0) = e^{-r\Delta t} \int_a^b C(y,T) \sum_{k=0}^{\infty}{}' A_k(x) \cdot \cos(k\pi\frac{y-a}{b-a}) dy \tag{36}$$

We interchange the summation and integration, and insert the definition

$$V_k := \frac{2}{b-a} \int_a^b C(y,T) \cos(k\pi\frac{y-a}{b-a}) dy \tag{37}$$

resulting

$$C_1(x,t_0) = \frac{1}{2}(b-a)e^{-r\Delta t} \cdot \sum_{k=0}^{\infty}{}' A_k(x)V_k \tag{38}$$

We further truncate the series summation to obtain approximation C_2 :

$$C_2(x,t_0) = \frac{1}{2}(b-a)e^{-r\Delta t} \cdot \sum_{k=0}^{N-1}{}' A_k(x)V_k \tag{39}$$

Replacing $A_k(x)$ in equation (39) by $F_k(x)$ as defined in equation (30), we finally obtain

$$C(x,t_0) \approx C_3(x,t_0) = e^{-r\Delta t}\sum_{k=0}^{N-1}{}' \mathrm{Re}\left\{\phi\left(\frac{k\pi}{b-a};x\right)\cdot\exp\left(-i\frac{ka\pi}{b-a}\right)\right\}V_k \tag{40}$$

which is the COS formula for general underlying processes.

4.2 Truncation range

The formula for the truncation range $[a,b]$ in the COS method is given by equation (11) in [3]:

$$[a,b] = \left[(x_0+c_1) - L\sqrt{c_2+\sqrt{c_4}},\ (x_0+c_1)+L\sqrt{c_2+\sqrt{c_4}}\right] \text{ with } L=10 \tag{41}$$

Here, $x_0 = log(S_0/K)$. c_n is the n-th cumulant of $x = \log(S_T/K)$ which is equal to the n-th derivative of the cumulant-generating function $g(\omega) = \log(E(e^{\omega x}))$ evaluated at $\omega = 0$. L is a constant set according to different models. For most models, L with values around 8 to 10 is enough to produce very accurate results.

For Heston model, c_1 and c_2 are given in Table 11 in [3]. According to [3], since the analytic formula of c_4 is too lengthy, it is omitted and a larger L is used. c_2 may become negative when the Feller condition ($2\kappa\theta > \sigma^2$) for the parameters is not satisfied, so the absolute value of c_2 is used. The truncation range $[a,b]$ for Heston model thus reads

$$[a,b] = \left[(x_0+c_1) - L\sqrt{|c_2|},\ (x_0+c_1)+L\sqrt{|c_2|}\right] \text{ with } L=12 \tag{42}$$

In the case with multiple maturities, however, not only c_2, but also c_4 may play an important role which cannot be justifiably omitted. However, the derivation of these cumulants becomes even more complicated. The analytic formula of c_1 may already be very lengthy, not to mention c_2 and c_4. We therefore use the finite difference method to get these values.

The cumulant-generating function $g(\omega)$ is closely related to the characteristic function $\phi(\omega)$:

$$g(\omega) = \log(E(e^{\omega x})) = \log(\phi(-i\omega)) \tag{43}$$

Thus, the derivative of the cumulant-generating functions can be derived as follows:

$$g'(\omega) = \frac{1}{\phi(-i\omega)}\frac{d\phi(-i\omega)}{d\omega} \tag{44}$$

$$g''(\omega) = -\frac{1}{\phi(-i\omega)^2}[\frac{d\phi(-i\omega)}{d\omega}]^2 + \frac{1}{\phi(-i\omega)}\frac{d^2\phi(-i\omega)}{d\omega^2} \tag{45}$$

$$g^{(3)}(\omega) = \frac{2}{\phi(-i\omega)^3}[\frac{d\phi(-i\omega)}{d\omega}]^3 - \frac{3}{\phi(-i\omega)^2}\frac{d\phi(-i\omega)}{d\omega}\frac{d^2\phi(-i\omega)}{d\omega^2} + \frac{1}{\phi(-i\omega)}\frac{d^3\phi(-i\omega)}{d\omega^3} \tag{46}$$

$$\begin{aligned} g^{(4)}(\omega) = &-\frac{6}{\phi(-i\omega)^4}[\frac{d\phi(-i\omega)}{d\omega}]^4 + \frac{12}{\phi(-i\omega)^3}[\frac{d\phi(-i\omega)}{d\omega}]^2\frac{d^2\phi(-i\omega)}{d\omega^2} - \frac{3}{\phi(-i\omega)^2}[\frac{d^2\phi(-i\omega)}{d\omega^2}]^2 \\ &- \frac{4}{\phi(-i\omega)^2}\frac{d\phi(-i\omega)}{d\omega}\frac{d^3\phi(-i\omega)}{d\omega^3} + \frac{1}{\phi(-i\omega)}\frac{d^4\phi(-i\omega)}{d\omega^4} \end{aligned} \tag{47}$$

Using finite difference methods, we can obtain the central difference approximation for the derivatives of the characteristic function:

$$\left.\frac{d\phi(-i\omega)}{d\omega}\right|_{\omega=0} \approx \frac{1}{\Delta\omega}[\phi(-i\frac{\Delta\omega}{2}) - \phi(i\frac{\Delta\omega}{2})] \tag{48}$$

$$\left.\frac{d^2\phi(-i\omega)}{d\omega^2}\right|_{\omega=0} \approx \frac{1}{(\Delta\omega)^2}[\phi(-i\Delta\omega) - 2 + \phi(i\Delta\omega)] \tag{49}$$

$$\left.\frac{d^3\phi(-i\omega)}{d\omega^3}\right|_{\omega=0} \approx \frac{1}{(\Delta\omega)^3}[\phi(-i\frac{3\Delta\omega}{2}) - 3\phi(-i\frac{\Delta\omega}{2}) + 3\phi(i\frac{\Delta\omega}{2}) - \phi(i\frac{3\Delta\omega}{2})] \tag{50}$$

$$\left.\frac{d^4\phi(-i\omega)}{d\omega^4}\right|_{\omega=0} \approx \frac{1}{(\Delta\omega)^4}[\phi(-i2\Delta\omega) - 4\phi(-i\Delta\omega) + 6 - 4\phi(i\Delta\omega) + \phi(i2\Delta\omega)] \tag{51}$$

Thus, the cumulants can be approximated:

$$c_1 = g'(\omega)|_{\omega=0} = \left.\frac{d\phi(-i\omega)}{d\omega}\right|_{\omega=0} \tag{52}$$

$$c_2 = g''(\omega)|_{\omega=0} = \left.\left[-\left(\frac{d\phi(-i\omega)}{d\omega}\right)^2 + \frac{d^2\phi(-i\omega)}{d\omega^2}\right]\right|_{\omega=0} \tag{53}$$

$$\begin{aligned} c_4 = g^{(4)}(\omega)|_{\omega=0} = \Bigg[&-6\left(\frac{d\phi(-i\omega)}{d\omega}\right)^4 + 12\left(\frac{d\phi(-i\omega)}{d\omega}\right)^2\cdot\frac{d^2\phi(-i\omega)}{d\omega^2} - 3(\frac{d^2\phi(-i\omega)}{d\omega^2})^2 \\ &-4\frac{d\phi(-i\omega)}{d\omega}\cdot\frac{d^3\phi(-i\omega)}{d\omega^3} + \frac{d^4\phi(-i\omega)}{d\omega^4}\Bigg]\Bigg|_{\omega=0} \end{aligned} \tag{54}$$

With c_1, c_2 and c_4 in hand, we can now calculate the truncation range according to equation (41). However, instead of using equation (41) directly, we use equation (42), but with L dependent on c_4:

$$L = \max\left\{16,\ 8\sqrt{\sqrt{|c_4|}/|c_2|}\right\} \tag{55}$$

Here, both the absolute values of c_2 and c_4 are used in case the Feller condition does not satisfy. When c_4 is small, this is equivalent to equation (42) with $L = 16$; when c_4 is large, it is equivalent to equation (41) with $L = 8$.

4.3 Number of terms in the truncated series

In equation (39), we truncate the series and use the first N terms to calculate the option prices. The larger the N, the more accurate the price but also the longer the computation time. Hence, we need to find a compromise between the speed and accuracy.

As shown in Table 5 of [3], $N = 128$ produces an error less than 10^{-9} in the Heston model with the parameters chosen there. However, in our case, with a larger L and multiple maturities, $N = 128$ might not be enough. Since we don't know how large N should be in advance, we start with a relatively small N, do the calibration, check the model output using a large N (say 1024) and redo the calibration with a larger N if the error exceeds a certain level.

Since the complexity of the COS method is $O(N \log_2(N))$, we set an upper bound (normally 1024) on N to avoid too expensive calculations. If a very large value of N is indeed needed, we will check the parameters to see whether it can be avoided.

5 Calibration

In order to be able to use the model for option pricing, its parameters have to be adjusted to the current market conditions as reflected in the implied volatility. Thus, having chosen a set of n market instruments (typically, call options) with strikes $\{K_1, K_2, ..., K_n\}$ and maturities $\{\tau_1, \tau_2, ..., \tau_n\}$, whose market prices are $\{C_1, C_2, ..., C_n\}$, the calibration is performed by minimizing the difference between the market data and the model output.

Usually, the cost function can be either the sum of the least-square absolute errors or the sum of the least-square relative errors. The former one implicitly assigns more weight to the expensive options (ITM and ATM options), and less weight to the OTM options. In our case, we have one ATM option and several OTM options (25-Δ call and 25-Δ put usually) and we certainly want to assign more weight to the ATM option. (Of course, we can use the 75-Δ call instead of the 25-Δ put since they have the same volatility, but this will result in a much larger price range, which might lead to greater error in the minimization procedure. That is why the 75-Δ call is never used.) Hence, the cost function is set as:

$$F = \sum_{i=1}^{n} w_i [C(S, K_i, \tau_i) - C_i]^2 \tag{56}$$

where $\{w_1, ...w_n\}$ is a chosen set of weights and $C(S, K, \tau)$ is calculated according to equation (40) where $x = \log(S/K)$. We choose uniform weights (with all the weights w_i set to 1) in the following tests.

Since we calibrate to the market data maturity by maturity, the cost function is hence minimized maturity by maturity. For each maturity, we have the quotes of ATM, 25-Δ RR and 25-Δ STR. We can then get the prices of 25-Δ call, ATM, and 25-Δ put as market prices in the cost function. Since the prices of the three options are of the same order of magnitude, there is actually not much difference in using absolute errors or relative errors in the cost function.

5.1 Minimization schemes

Generally, there are two different kinds of minimization schemes, namely local (deterministic) algorithms and global (stochastic) algorithms. Local algorithms depend largely on the initial guess and might easily fall into local minima. Stochastic algorithms will find a global minimum, but they are much more computationally burdensome.

Past researchers all emphasize on the importance of finding the global minimum in the calibration procedure. However, in our tests of the multi-period case, we find that the global minimum of one period does not necessarily produce nice results for the next period. It can happen that several completely different sets of parameters all produce prices close enough to the market data. In this case, it is certainly better to choose one set that is not extreme in value and relatively stable compared to the previous set.

Based on such consideration, I currently choose a local algorithm (the Matlab function, fminsearch, which uses the Nelder-Mead Simplex search method). Therefore, a set of good initial values needs to be found as input. For the first period, the initial parameters are set manually; for the later periods, the calibrated parameters of the previous period are used as the initial values for the next one. The local algorithm hence ensures the stability of the parameters.

5.2 Parameters and their initial values

In the Heston model, there are totally 5 free parameters, the mean reversion rate κ, volatility of variance σ (vol of vol), correlation ρ, initial variance V_0 and long run variance θ. Since three market prices (25-Δ call, ATM and 25-Δ put) are available for each maturity, two of the parameters have to be fixed.

Of the 5 parameters, κ is chosen manually. For the first period, we calibrate σ, ρ and V_0. θ is set equal to V_0 as many practitioners do. In the Dolphin implementation of the Heston Model [26], FX Quantitative Analytics set this coefficient of proportionality, θ/V_0, to 1.5. This is done in order to avoid negative prices in their model which includes the term structure adjustment. However, there is no convincing reason to do so otherwise. Thus we still stay with $\theta = V_0$, which also gives much freedom in the choice of κ.

For the later periods, since V_0 is already fixed, we calibrate θ instead (actually the coefficient of proportionality, θ/V_0, in the tests).

Since the local algorithm is chosen, the task now is to find a set of good initial values. It is not a good idea to just randomly choose several sets of initial parameters in the hope of finding the global minimum. Rather we can set them according to the information contained in the market data.

Since we have set θ equal to V_0 for the first period, the major contribution to the change of volatility comes from the stochastic part. Thus, we can imagine that the volatility might not fluctuate too much from its initial value, which indicates that we might just set V_0 to be the square of the ATM implied volatility of the first maturity. In our tests, we find that compared to the square of the ATM volatility, the calibrated V_0 is even closer to the square of the 25-Δ put volatility in a negatively skewed market, but it does not make much difference which we take as the initial value.

Next we consider the initial value of ρ. The RR contains information about the skewness, and consequently influences the value of the correlation. If the quote of RR is negative, i.e. the 25-Δ put has a higher volatility than the 25-Δ call, we then have a downward skew in the smile. Hence, ρ is negative in this case. A positive ρ will produce an upward skew in the smile. Thus, ρ has the same sign as RR [9]. Suppose that the term structure of RR implies an increasing skewness for longer maturities (since ATM volatilities also changes, it is better to divide the RR quote by the ATM quote when comparing skewness), a large initial value for ρ will not be suitable. If there is a local minimum close to the extreme value, the increasing skewness will drive ρ to -1 (or 1) in the calibration of later periods, resulting in the failure

of the calibration. Therefore, the initial value of ρ can vary, but it is usually chosen close to -0.5 (or 0.5). We set it to -0.4574 in our tests.

What remains to be determined is σ. Actually, σ and κ are actually strongly interdependent. While a large σ increases the volatility of v, a large κ will offset this effect. Thus, the combination of a large σ and a large κ can produce the same result as a small σ and a small κ.

If the Feller condition ($2\kappa\theta > \sigma^2$) does not satisfy, the variance process may become negative with a non-zero probability. This condition does not always hold (e.g. for very skewed markets), but it is certainly desired that it is satisfied. Thus, we can set the initial value of σ to be around $\sqrt{2\kappa\theta}$, using the initial values of κ and θ. If this initial value results in a local minimum, we will try larger values of σ in search of a global minimum.

Once the parameters of one period are calibrated, they are used as the initial input for the next period.

5.3 Mean reversion rate

The mean reversion rate κ is set manually before the calibration. In the Dolphin implementation for ordinary Heston model [26], it is set to 0.2. We will show that for the term structure Heston model, this value for the mean reversion rate is not always suitable, for every set of market data.

For the one-maturity calibration case, we find in the tests that if the model can be calibrated, then for any κ we take, we will always find a σ which suits the model (see section 5.2 for a theoretical explanation).

For the multi-period calibration case, this is no longer true. Imagine that the ATM volatility level (σ_2) at the second maturity falls dramatically from that of the first maturity. Suppose the length of the second period is short, then the chances that the volatility will reach the new level given a small κ are rather low. This can be seen more clearly if there is no volatility smile (that is, we remove the stochastic part of the volatility SDE and make it deterministic). In this case, the ATM variances at the first two maturities are as follows:

$$dv(t) = \kappa(\theta - v(t))dt \tag{57}$$

$$\Rightarrow v_{t_1} = (v_{t_0} - \theta_1)e^{-\kappa_1(t_1 - t_0)} + \theta_1 = \theta_1 \tag{58}$$

$$v_{t_2} = (v_{t_1} - \theta_2)e^{-\kappa_2(t_2 - t_1)} + \theta_2 = (\theta_1 - \theta_2)e^{-\kappa_2(t_2 - t_1)} + \theta_2 \tag{59}$$

Thus, the ATM volatility at the second maturity is

$$\sigma_2 = \left(\int_{t_0}^{t_1} v(s)ds + \int_{t_1}^{t_2} v(s)ds \right)^{\frac{1}{2}} / (t_2 - t_0)^{\frac{1}{2}} \tag{60}$$

$$= \left(\theta_1(t_1 - t_0) + \frac{\theta_1 - \theta_2}{\kappa_2}(1 - e^{-\kappa_2(t_2 - t_1)}) + \theta_2(t_2 - t_1) \right)^{\frac{1}{2}} / (t_2 - t_0)^{\frac{1}{2}} \tag{61}$$

$$> \left(\theta_1(t_1 - t_0) + \frac{\theta_1}{\kappa_2}(1 - e^{-\kappa_2(t_2 - t_1)}) \right)^{\frac{1}{2}} / (t_2 - t_0)^{\frac{1}{2}} \tag{62}$$

$$\Rightarrow \frac{\kappa_2}{1 - e^{-\kappa_2(t_2 - t_1)}} > \frac{\sigma_1^2}{\sigma_2^2(t_2 - t_0) - \sigma_1^2(t_1 - t_0)} \tag{63}$$

Since the left-hand-side is an increasing function of κ_2, this shows that for every ATM volatility value at the second maturity, κ_2 cannot be smaller than a certain value in order for the volatility to reach that level.

In the stochastic case, it is hard to get an analytic formula for the lower bound of κ_2. Although we do not know it exactly, we assume that the minimum value of κ_2 in the deterministic case can serve as a good reference on how large κ_2 should be in order to be calibrated, especially when there is no large smile.

6 Calibration results

We apply the piecewise constant calibration method to the EUR/USD market and USD/JPY market. The maturities taken into consideration range from 6-month to 5-year (including 9m, 1y, 2y, 3y and 4y). For each maturity, the market price of the 25-Δ call, ATM and 25-Δ put are available.

Since some parameters have constraints to satisfy, we thus use the technique of change of variables to avoid constrained optimization. Suppose the parameter p is bounded in the interval $[p_{min}, p_{max}]$, using an unconstrained parameter $\tilde{p}$, we can express p in terms of $\tilde{p}$ as

$$p = p_{min} + \frac{p_{max} - p_{min}}{2}\left(1 + \tanh(\frac{\tilde{p}}{100})\right) \tag{64}$$

This ensures that the parameter values stay within the proper range.

6.1 EUR/USD market

We first test the EUR/USD data listed in Table 38 on each single maturity. κ is set to 0.2 and 2 respectively. We set the number of terms in the truncated series of the COS method, N, to 256.

Period	0-6m	0-9m	0-1y	0-2y	0-3y	0-4y	0-5y
σ	0.2960	0.2536	0.2317	0.1692	0.1512	0.1341	0.1297
ρ	-0.1653	-0.1564	-0.1454	-0.1490	-0.1598	-0.1698	-0.1774
V_0	0.0262	0.0246	0.0239	0.0230	0.0222	0.0209	0.0199
(25-Δ put vol)^2	0.0257	0.0238	0.0228	0.0220	0.0210	0.0197	0.0186
(ATM vol)^2	0.0228	0.0210	0.0202	0.0195	0.0185	0.0174	0.0164
(25-Δ call vol)^2	0.0229	0.0214	0.0207	0.0201	0.0191	0.0179	0.0168
Max Rel. Error	2.89E-07	1.43E-07	1.45E-07	1.32E-07	8.79E-08	4.94E-08	1.12E-07
$c1$	-0.0121	-0.0168	-0.0220	-0.0424	-0.0610	-0.0766	-0.0907
$c2$	0.1144	0.1359	0.1562	0.2177	0.2634	0.2962	0.3250
$c4$	0.0006	0.0004	0.0013	0.0048	0.0109	0.0174	0.0286
L	16	16	16	16	16	16	16
$b-a$	3.6595	4.3488	4.9994	6.9665	8.4286	9.4770	10.3990

Table 2: Parameters calibrated to every single maturity of EUR/USD with $\kappa = 0.2$ and $N = 256$, market data in Table 38

The maximum relative error for each maturity τ is defined as:

$$\text{Max Rel. Error} = \max_{1\le i\le 3}\left|\frac{C^{model}(S, K_i, \tau) - C_i}{C_i}\right| \tag{65}$$

Period	0-6m	0-9m	0-1y	0-2y	0-3y	0-4y	0-5y
σ	0.4421	0.4518	0.4854	0.5200	0.5946	0.6171	0.6738
ρ	-0.1609	-0.1514	-0.1404	-0.1420	-0.1519	-0.1610	-0.1684
V_0	0.0265	0.0250	0.0246	0.0236	0.0228	0.0214	0.0204
Max Rel. Error	7.12E-08	6.10E-08	5.10E-08	9.41E-08	1.02E-07	1.27E-07	1.03E-07
$c1$	-0.0121	-0.0170	-0.0224	-0.0431	-0.0619	-0.0776	-0.0918
$c2$	0.1152	0.1375	0.1587	0.2216	0.2686	0.3015	0.3309
$c4$	0.0001	0.0017	0.0018	0.0076	0.0195	0.0293	0.0470
L	16	16	16	16	16	16	16
$b-a$	3.6850	4.3988	5.0791	7.0915	8.5963	9.6490	10.5882

Table 3: Parameters calibrated to every single maturity of EUR/USD with $\kappa = 2$ and $N = 256$, market data in Table 38

where $C_i, i = 1, 2, 3$ are the market data and $C^{model}(S, K_i, \tau), i = 1, 2, 3$ are the model outputs using the calibrated parameters.

From Table 2 and Table 3, we see that in both cases, all the maturities can be calibrated well. $V_0 (= \theta)$ is closer to the square of the 25-Δ put volatility (less than 10% difference) than that of the ATM volatility. ρ is not large as the EUR/USD market is not a severely skewed one. When we increase κ from 0.2 to 2, ρ and V_0 change very slightly, but σ increases with κ, as pointed out in section 5.2.

All the relative pricing errors are below 10^{-6} and each calibration is done within a couple of seconds. This shows that the calibration method is fast and accurate in the single maturity cases.

Period	0-6m	6m-9m	9m-1y	1y-2y	2y-3y	3y-4y	4y-5y
σ	0.4421	0.1405	1.4122	0.4311	0.9182	0.5643	1.3646
ρ	-0.1609	-0.0878	-0.0916	-0.2105	-0.1674	-0.2445	-0.2037
V_0	0.0265						
θ/V_0	1	0.1770	1.6070	0.8000	0.7735	0.5713	0.6519
Max Rel. Error	7.12E-08	1.58E-09	1.15E-08	4.06E-07	9.34E-08	8.05E-08	6.85E-08
$c1$	-0.0121	-0.0170	-0.0224	-0.0438	-0.0626	-0.0785	-0.0930
$c2$	0.1152	0.1372	0.1586	0.2259	0.2726	0.3066	0.3369
$c4$	0.0001	0.0008	0.0023	0.0142	0.0284	0.0471	0.0710
L	16	16	16	16	16	16	16
$b-a$	3.6850	4.3900	5.0757	7.2290	8.7236	9.8103	10.7813

Table 4: Parameters calibrated to multiple maturities of EUR/USD with $\kappa = 2$ and $N = 256$, market data in Table 38

	ini value 1	calibrated	ini value 2	calibrated	ini value 3	calibrated
σ	1.3646	20	0.5643	20	1.4122	20
ρ	-0.2037	0.99	-0.2444	0.99	-0.0916	0.99
θ/V_0	0.6519	0.2367	0.5713	0.2366	1.6070	0.2366

Table 5: Initial parameters tried for maturity 6y to calibrate that maturity in the multiple maturity calibration of EUR/USD with $\kappa = 2$ and $N = 512$, market data in Table 38

Next we calibrate to the multiple maturities, starting from 6-month till 5-year. We calibrate maturity by maturity. When the previous maturity is calibrated and the parameters fixed, we calibrate to the market data of the next maturity and find the corresponding parameters. If we set κ to 0.2, we find that the calibration fails when calibrating to the data of the second maturity (i.e. 9-month). This shows that there is indeed a minimum on the value of κ in the stochastic case as well. As discussed in Section 5.3, when the volatility is deterministic, we find κ to be at least 2.3, but in the stochastic case, it has a different range. When we increase κ to 2, we find that all the 7 maturities can be calibrated well (see Table 4). In this case, θ for the second period is rather low, which shows that in compensation for a low κ, the level of the long term variance has to be reduced dramatically in order to reach a lower volatility level at the second maturity. If we increase κ to 5, θ turns out to be around $0.6V_0$ in the second period.

For the calibrated parameters, we find $L = 16$ for all options and all maturities. This shows that c_4 is very small and can be omitted in the calibration of EUR/USD options.

The multiple maturities from 1-month to 5-year can also be calibrated, but in this case κ has to be set to 15, which seems somehow impractical.

However, when we try to calibrate to the maturities from 6m to 6y, we find that we cannot get proper parameters for the last maturity (see Table 5). The calibrated parameters of several previous maturities have been tried as the initial values for the last maturity. However, the parameters will go to very extreme values (σ to the upper bound we set and ρ to 1) no matter we set N to 256 or 512, indicating failure in finding the minimum. The resulting maximum error is about 1%. This suggests that the successful calibration also depends on the market data and the SDE model chosen.

6.2 USD/JPY market

Next we test the USD/JPY data listed in Table 39. Since USD/JPY market is a highly skewed one, it can be tougher to handle than the EUR/USD market.

We still start tests on each single maturity. κ is again set to 0.2 (see Table 6) and 2 (see Table 7) respectively. In both cases, $N = 256$ works well for the first several maturities, but for the last several maturities, N has to be increased to 512. This results from a larger c_4 and hence a larger value of L in the truncation range, bringing more computational burden. It

Period	0-6m	0-9m	0-1y	0-2y	0-3y	0-4y	0-5y
σ	0.2818	0.2614	0.2590	0.2125	0.2221	0.2536	0.2890
ρ	-0.5448	-0.5684	-0.5888	-0.6349	-0.6767	-0.6763	-0.6874
V_0	0.0151	0.0150	0.0155	0.0148	0.0157	0.0177	0.0198
(25-Δ put vol)^2	0.0171	0.0169	0.0171	0.0164	0.0166	0.0172	0.0176
(ATM vol)^2	0.0124	0.0117	0.0114	0.0103	0.0099	0.0100	0.0101
(25-Δ call vol)^2	0.0098	0.0090	0.0086	0.0072	0.0065	0.0065	0.0064
Max Rel. Error	5.80E-08	1.49E-07	3.19E-07	7.28E-07	2.72E-06	1.81E-06	8.65E-07
$c1$	-0.0007	-0.0012	-0.0020	-0.0045	-0.0087	-0.0154	-0.0242
$c2$	0.0879	0.1083	0.1292	0.1829	0.2391	0.3055	0.3794
$c4$	-0.0002	0.0007	0.0014	0.0106	0.0441	0.1654	0.5327
L	16.00	16.00	16.00	16.00	16.00	16.70	18.01
$b-a$	2.81	3.46	4.13	5.85	7.65	10.20	13.67
N	256	256	256	256	512	512	512

Table 6: Parameters calibrated to every single maturity of USD/JPY with $\kappa = 0.2$, market data in Table 39

Period	0-6m	0-9m	0-1y	0-2y	0-3y	0-4y	0-5y
σ	0.4134	0.4673	0.5641	0.7133	0.9906	1.3605	1.7376
ρ	-0.5504	-0.5727	-0.5903	-0.6311	-0.6701	-0.6672	-0.6782
V_0	0.0154	0.0156	0.0166	0.0162	0.0177	0.0201	0.0224
Max Rel. Error	1.36E-07	1.46E-06	9.01E-06	2.30E-05	1.20E-05	6.05E-06	7.28E-06
$c1$	-0.0007	-0.0014	-0.0025	-0.0059	-0.0116	-0.0201	-0.0306
$c2$	0.0890	0.1111	0.1351	0.1966	0.2649	0.3461	0.4351
$c4$	-0.0006	0.0013	0.0036	0.0296	0.1606	0.6846	2.2548
L	16	16	16	16.88	19.12	21.03	22.53
$b-a$	2.85	3.55	4.32	6.64	10.13	14.55	19.61
N	256	256	256	256	512	512	512

Table 7: Parameters calibrated to every single maturity of USD/JPY with $\kappa = 2$, market data in Table 39

thus suggests that we should consider a small value of κ in the multiple-maturity calibration in view of computational speed.

From Table 6, we can see that again $V_0 (= \theta)$ are quite close to the square of the 25-Δ put volatilities (about 10% difference). For long maturities, there are dramatic increases in the values of σ when we increase κ from 0.2 to 2, which results in large c_4. The errors are also relatively large in the latter case.

Period	0-6m	6m-9m	9m-1y	1y-2y	2y-3y	3y-4y	4y-5y
κ	2	2	2	2	2	2	2
σ	0.4134	1.0216	2.7734	0.7215	3.8857	15.1340	15.1983
ρ	-0.5504	-0.6283	-0.7085	-0.8364	-0.8339	-0.7203	-0.7902
V_0	0.0154						
θ/V_0	1	1.3611	3.3761	0.8466	2.7452	7.8526	7.5280
Max Rel. Error	1.36E-07	3.85E-06	7.34E-05	2.41E-05	2.06E-05	4.20E-05	7.99E-04
$c1$	-0.0007	-0.0015	-0.0034	-0.0093	-0.0201	-0.0572	-0.1076
$c2$	0.0890	0.1119	0.1455	0.2325	0.3523	0.9418	1.6947
$c4$	0.0005	0.0022	0.0145	0.2151	2.3652	1316.72	16183.31
L	16	16	19.08	23.44	28.16	51.17	53.24
$b-a$	2.85	3.58	5.55	10.90	19.84	96.38	180.46
N	256	256	256	512	1024	2048	2048

Table 8: Parameters calibrated to multiple maturities of USD/JPY, $\kappa = 2$, market data in Table 39

Period	0-6m	6m-9m	9m-1y	1y-2y	2y-3y	3y-4y	4y-5y
κ	2	2	2	2	1	0.5	0.5
σ	0.4134	1.0216	2.7734	0.7215	2.2016	3.7831	3.3951
ρ	-0.5504	-0.6283	-0.7085	-0.8364	-0.8282	-0.7041	-0.7976
V_0	0.0154						
θ/V_0	1	1.3611	3.3761	0.8466	3.0592	7.8223	6.6708
Max Rel. Error	1.36E-07	3.85E-06	7.34E-05	2.41E-05	8.83E-06	1.15E-05	7.23E-05
$c1$	-0.0007	-0.0015	-0.0034	-0.0093	-0.0183	-0.0398	-0.0724
$c2$	0.0890	0.1119	0.1455	0.2325	0.3283	0.5504	0.8990
$c4$	0.0005	0.0022	0.0145	0.2151	1.0720	22.90	278.32
L	16	16	19.08	23.44	24.80	31.80	36.34
$b-a$	2.85	3.58	5.55	10.90	16.28	35.00	65.35
N	256	256	256	512	1024	1024	1024

Table 9: Parameters calibrated to multiple maturities from 6m to 5y of USD/JPY, varying κ, market data in Table 39

When we calibrate to the multiple maturities, we have to be very careful in choosing κ in this case. For the first several periods, we need a relatively large κ to match the volatility term structure, but we need to decrease it in the later periods to avoid a very large truncation range.

When we set κ to 2 for all intervals, σ turns out to be very large in the last several intervals

(see Table 8). A very large N (at least 2048) is hence needed in COS pricing for the successful calibration, which significantly increases the time. Through trial and error, we decrease κ for the last 3 maturities as shown in Table 9 and manage to control the value of σ within a reasonable range. With N set to 256 in the first period and gradually increased to 1024 in the last several periods, we get the parameters which produce relative errors less than 10^{-4}. The upper bound of N is set to 1024 in concern of the computation time.

We also try to calibrate from 6m to 10y. From Table 10, we see that for the maturity of 7y, we do not obtain a good set of parameters (σ and θ/V_0 become unreasonably large). Hence, for this and consequent maturities, there are relatively large errors between the model output and market data. Larger N has also been tried, but doesn't give a good set of parameters either.

Period	0-6m	6m-9m	9m-1y	1y-2y	2y-3y	3y-4y
κ	2	2	2	2	1	0.5
σ	0.4134	1.0216	2.7734	0.7215	2.2016	3.7830
ρ	-0.5504	-0.6283	-0.7085	-0.8364	-0.8282	-0.7041
V_0	0.0154					
θ/V_0	1	1.3611	3.3761	0.8466	3.0592	7.8221
Max Rel. Error	1.36E-07	3.85E-06	7.34E-05	2.41E-05	8.83E-06	1.19E-05
$c1$	-0.0007	-0.0015	-0.0034	-0.0093	-0.0183	-0.0398
$c2$	0.0890	0.1119	0.1455	0.2325	0.3283	0.5504
$c4$	0.0005	0.0022	0.0145	0.2151	1.0720	22.8984
L	16	16	19.08	23.44	24.80	31.80
$b-a$	2.85	3.58	5.55	10.90	16.28	35.00
N	256	256	256	512	1024	2048
Period	4y-5y	5y-6y	6y-7y	7y-8y	8y-9y	9y-10y
κ	0.5	0.5	0.5	0.5	0.5	0.5
σ	3.3799	3.3788	16.7917	1.9063	3.0063	12.3797
ρ	-0.7975	-0.8045	-0.6602	-0.7139	-0.5648	-0.4686
θ/V_0	6.6418	7.1198	29.6627	7.7974	9.3465	38.4467
Max Rel. Error	1.46E-05	1.26E-05	1.50E-03	2.11E-02	3.71E-02	3.78E-02
$c1$	-0.0723	-0.1099	-0.1865	-0.2753	-0.3463	-0.4547
$c2$	0.8985	1.2761	2.3635	4.2620	5.6015	6.6733
$c4$	277.35	1322.32	39584	784900	2660684	5238217
L	36.34	37.80	47.74	55.87	57.68	57.35
$b-a$	65.29	96.48	225.68	476.24	646.20	765.45
N	2048	2048	2048	2048	2048	2048

Table 10: Parameters calibrated to multiple maturities from 6m to 10y of USD/JPY, varying κ, market data in Table 39 (Note: the parameters till 5y are the same as those in Table 9)

7 Historic tests

In this section, we test our term structure Heston model by calibrating it to some historic data spanning a whole year. In this way, we can see whether our model is sufficiently robust in the calibration so as to be used in pricing exotic options. Before we do the historic tests, we first perform some jump tests on the historic market data based on some test statistics to see whether there are jumps or not in the data, since our model does not assume jumps.

7.1 Jump tests on market data

7.1.1 Jump tests in a discretely observed process

The problem of deciding whether the continuous-time process which models a financial time series should have continuous paths or exhibit jumps is becoming an increasingly important issue, in view of the high-frequency observations that are now widely available [20].

Two closely related but different issues are to decide whether jumps are present or not and to determine the impact of jumps on the overall variability of the observed process. Most of the literature so far has concentrated on the second issue [20]. Until recently, Ait-Sahalia and Jacod [20] propose a method to determine whether jumps are present or not in discretely sampled processes. As the sampling interval tends to 0, the test statistic converges to 1 if there are jumps, and to another deterministic and known value (such as 2) if there are no jumps. We want to use their test method to see whether the Heston model (without jumps) we choose is suitable for the EUR/USD and USD/JPY markets or not.

In the case where a large jump occurs, a simple glance at the data set might be sufficient to decide on this issue, but small or medium sized jumps are much more difficult to distinguish visually. Hence, it is important to have some statistical methods.

Assume that X is an Itô semimartingale on some filtered space $(\Omega, \mathcal{F}, (\mathcal{F}_t)_{t\geq 0}, \mathbb{P})$:

$$\begin{aligned} X_t =& X_0 + \int_0^t b_s ds + \int_0^t \sigma_s dW_s + \int_0^t \int_E g \circ \delta(s,x)(\mu - \nu)(ds,dx) \\ &+ \int_0^t \int_E g' \circ \delta(s,x)\mu(ds,dx) \end{aligned} \tag{66}$$

where W is a Wiener process, μ is a Poisson random measure on $R_+ \times E$ with $(E, \mathcal{E})$ an auxiliary measurable space on the space $(\Omega, \mathcal{F}, (\mathcal{F}_t)_{t\geq 0}, \mathbb{P})$ and the predictable compensator (or intensity measure) of μ is $\nu(ds, dx) = ds \otimes \lambda(dx)$ for some given finite or σ-finite measure on $(E, \mathcal{E})$. Moreover g is a continuous function with compact support and $g(x) = x$ on a neighborhood of 0, and $g'(x) = x - g(x)$.

σ_t is also an Ito semimartingale, of the form

$$\begin{aligned} \sigma_t =& \sigma_0 + \int_0^t \widetilde{b}_s ds + \int_0^t \widetilde{\sigma}_s dW_s + \int_0^t \widetilde{\sigma}'_s dW'_s + \int_0^t \int_E g \circ \widetilde{\delta}(s,x)(\mu - \nu)(ds,dx) \\ &+ \int_0^t \int_E g' \circ \widetilde{\delta}(s,x)\mu(ds,dx) \end{aligned} \tag{67}$$

where W' is another Wiener process independent of (W, μ).

In addition, we write

$$\Delta X_s = X_s - X_{s-} \tag{68}$$

Clearly, $\Delta X_s = 0$ for all s when X is continuous.

Our process X is discretely observed over a given time interval $[0, t]$. Suppose that X can be observed at times $i\Delta_n$ for all $i = 0, 1, ..., [t/\Delta_n]$, where $[\cdot]$ is the ceil function. As $n \to \infty$, $\Delta_n \to 0$.

Now we define a number of processes which all measure some kind of variability of X, or perhaps its continuous and jump components separately, and depend on the whole (unobserved) path of X:

$$A(p)_t = \int_0^t |\sigma_s|^p ds \tag{69}$$

$$B(p)_t = \Sigma_{s \le t} |\Delta X_s|^p \tag{70}$$

where p is a positive number.

In the actual observations, let

$$\Delta_i^n X = X_{i\Delta_n} - X_{(i-1)\Delta_n} \tag{71}$$

denote the observed discrete increments of X and define for $p > 0$ the estimator

$$\widehat{B}(p, \Delta_n)_t = \Sigma_{i=1}^{t/\Delta_n} |\Delta_i^n X|^p \tag{72}$$

For $r \in (0, \infty)$, let

$$m_r = E(|U|^r) = \pi^{-1/2} 2^{r/2} \Gamma\left(\frac{r+1}{2}\right) \tag{73}$$

denote the rth absolute moment of a variable $U \sim N(0, 1)$. We have the following convergences in probability, locally uniform in t:

$$\begin{cases} p > 2 & \Rightarrow \quad \widehat{B}(p, \Delta_n)_t \xrightarrow{\mathbb{P}} B(p)_t \\ p = 2 & \Rightarrow \quad \widehat{B}(p, \Delta_n)_t \xrightarrow{\mathbb{P}} [X, X]_t \\ p < 2 & \Rightarrow \quad \frac{\Delta_n^{1-p/2}}{m_p} \widehat{B}(p, \Delta_n)_t \xrightarrow{\mathbb{P}} A(p)_t \\ X \text{ is continuous} & \Rightarrow \quad \frac{\Delta_n^{1-p/2}}{m_p} \widehat{B}(p, \Delta_n)_t \xrightarrow{\mathbb{P}} A(p)_t \end{cases} \tag{74}$$

where $[X, X]_t$ is the quadratic variation.

The intuition for the behavior of $\widehat{B}(p, \Delta_n)_t$ is as follows. Suppose X can jump. While the increments of X containing large jumps are much less frequent than those small ones, they are so much bigger in magnitude that they overwhelm $B(p)$ when $p > 2$, since large values are magnified and small ones suppressed. When p is small ($p < 2$), the sum is driven by the summation of the small increments since the magnification of the large jumps is not strong enough to suppress all the other small ones. When $p = 2$, these two effects (magnification of

the relatively few large increments vs. summation of many small increments) are of the same magnitude. When X is continuous, there are no large jumps and we are in the same situation as $p < 2$.

Based on this intuition, we see when $p > 2$ the limit of $\widehat{B}(p, \Delta_n)_t$ does not depend on the sequence Δ_n going to 0, and it is strictly positive if X has jumps between 0 and t. On the other hand, when X is continuous on $[0, t]$, $\widehat{B}(p, \Delta_n)_t$ converges again to a limit not depending on Δ_n, but only after a normalization which depends on Δ_n.

We set

$$\widehat{S}(p, k, \Delta_n)_t = \frac{\widehat{B}(p, k\Delta_n)_t}{\widehat{B}(p, \Delta_n)_t} \tag{75}$$

where k is an integer.

Let $t > 0$, $p > 2$ and $k \geq 2$. Then

$$\widehat{S}(p, k, \Delta_n)_t \xrightarrow{\mathbb{P}} S(p, k)_t = \begin{cases} 1, & on\ the\ set\ \Omega_t^j \\ k^{p/2-1}, & on\ the\ set\ \Omega_c^j\ (for\ p\ \leq\ 2\ as\ well) \end{cases} \tag{76}$$

Therefore the test statistics will converge to 1 in the presence of jumps and, with the selection of $p = 4$ and $k = 2$, to 2 in the absence of jumps.

The decision rule is defined by:

$$\begin{cases} X\ is\ discontinuous\ on\ [0, t], & if\ \widehat{S}(p, k, \Delta_n)_t < a \\ X\ is\ continuous\ on\ [0, t], & if\ \widehat{S}(p, k, \Delta_n)_t \geq a \end{cases} \tag{77}$$

for certain choice of a in the interval $(1, k^{p/2} - 1)$.

7.1.2 Jump tests in EUR/USD and USD/JPY historic data

Now we apply the statistical method to the EUR/USD historic data. We take the FX spot from Sep. 1, 1998 to Aug. 31, 2008.

In Table 11, we can see that when k is set to 2, $\widehat{S}(p, k, \Delta_n)_t = 1.69$, which is closer to the limit 2 corresponding to the continuous case. So are the cases where $k = 5$ and $k = 10$. Although we have not got the confidence interval (which is quite complicated), we are quite sure that the probability that there are no jumps in the EUR/USD market during that period is high.

Next we apply the statistical method to the USD/JPY historic data. We also take the FX spot from Sep. 1, 1998 to Aug. 31, 2008.

In Table 12, we can see that when k is set to 2, $\widehat{S}(p, k, \Delta_n)_t = 0.52$, well below the theoretical limit 1, which corresponds to the discontinuous case. Clearly, jumps exist in the USD/JPY spot process. This can be verified when we set $k = 5$ and $k = 10$. The results (2.02 and 2.18) are again far closer to the theoretic limit in the discontinuous case rather than the continuous case. Hence even without the confidence interval, we are quite sure that the probability that there are jumps in the USD/JPY market during that period is high.

Figure 1: EUR/USD spot from Sep. 1, 1998 to Aug. 31, 2008

p=4	k=1	k=2	k=5	k=10
$\widehat{B}(p, k\Delta_n)_t$	2.19E-05	3.70E-05	7.48E-05	1.69E-04
$\widehat{B}(p, k\Delta_n)_t / \widehat{B}(p, \Delta_n)_t$	/	1.69	3.42	7.72
theoretic limit if continuous	/	2	5	10
theoretic limit if discontinuous	/	1	1	1

Table 11: The test statistics for EUR/USD historic data from Sep. 1, 1998 to Aug. 31, 2008

Therefore, models with jumps (e.g. Bates' model) might be preferred for USD/JPY market instead of models without jumps (e.g. Heston model).

What is worth mentioning here is that we used historic data before the deterioration of the current financial crisis. Since then, the FX market has become extremely volatile and even EUR/USD has become an emerging-market-like currency. If we test the data in that period, we think the results will very likely indicate jumps. However, since the size of the sample space is too small, it might not be very meaningful from the statistics point of view.

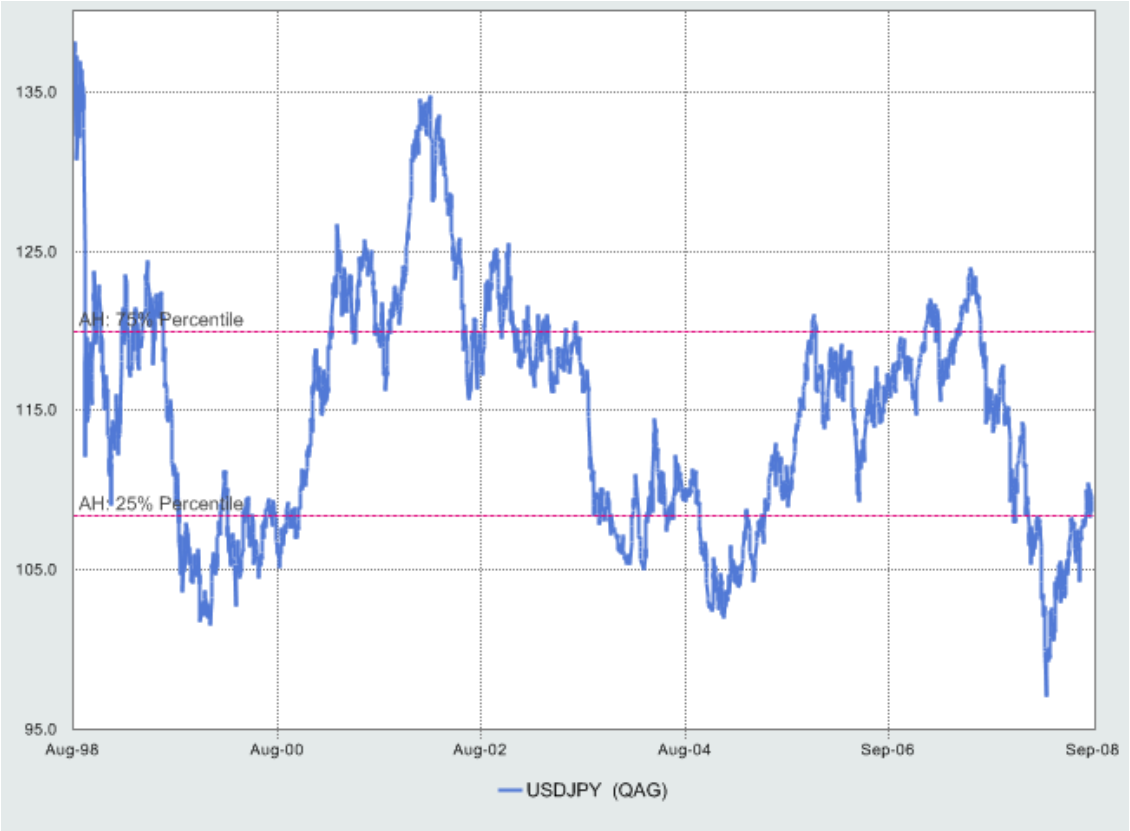

Figure 2: USD/JPY spot from Sep. 1, 1998 to Aug. 31, 2008

p=4	k=1	k=2	k=5	k=10
$\widehat{B}(p, k\Delta_n)_t$	3.58E+04	1.85E+04	7.23E+04	7.81E+04
$\widehat{B}(p, k\Delta_n)_t / \widehat{B}(p, \Delta_n)_t$	/	0.52	2.02	2.18
theoretic limit if continuous	/	2	5	10
theoretic limit if discontinuous	/	1	1	1

Table 12: The test statistics for USD/JPY historic data from Sep. 1, 1998 to Aug. 31, 2008

7.2 Calibration using historic data

Since it seems that models without jumps might apply for the EUR/USD market, we calibrate the TS Heston model to the EUR/USD historic data (the quotes of spot, ATM, 25-Δ RR and 25-Δ STR) to see whether the calibrations will be successful and whether the TS parameters are stable.

We test on the EUR/USD historic data starting from Sep. 3, 2007 to Aug. 29, 2008. Since the 9m market data are not available, we use maturities 6m, 1y, 2y, 3y, ..., 9y and 10y, eleven maturities in total. Hence we have 11 periods in our term structure: period 1 (0 - 6m),

period 2 (6m - 1y), period 3 (1y - 2y), ..., period 10 (8y - 9y) and period 11 (9y - 10y). Since in the previous test, the calibration breaks down when we try to calibrate the period from 5y to 6y, we expect similar results in the historic test as well.

Period No	Num of days calibration fails	Percentage
Period 1 (0 - 6m)	0	0.00%
Period 2 (6m - 1y)	0	0.00%
Period 3 (1y - 2y)	0	0.00%
Period 4 (2y - 3y)	2	0.78%
Period 5 (3y - 4y)	0	0.00%
Period 6 (4y - 5y)	43	16.67%
Period 7 (5y - 6y)	158	61.24%
Period 8 (6y - 7y)	5	1.94%
Period 9 (7y - 8y)	0	0.00%
Period 10 (8y - 9y)	2	0.78%
Period 11 (9y - 10y)	2	0.78%
Num of days calibration succeeds till final maturity		
46		17.83%

Table 13: The periods where calibration breaks down

The calibration results do not go beyond our expectations. Of all the 258 trading days in that year, calibration breaks down in period 7 (5y - 6y) on 158 days. The number of failures in period 4 (2y - 3y) is 2, in period 6 (4y - 5y) is 43, in period 8 (6y - 7y) is 5, in period 10 (8y - 9y) is 2 and in period 11 (9y - 10y) is 2 as well. On the other days (46 in total), the calibration is successful till the final maturity.

The results again suggest that the success of calibration depends on the market data. One case that the calibration might break down is when the volatility surface is downward sloping with time and there is some relatively large downward jump at certain long maturity. We think that the large jump in the volatility level might require a very large mean reversion rate (or a very low mean reversion level) and hence results in the failure of the calibration. In a correspondence with Alberto Elices, the author of [4], he also agrees: "I agree with you that not every possible market data might be calibrated with a Heston model with time dependent parameters. The bootstrapping algorithm that is proposed in the paper does an optimization of four parameters at each maturity. This calibration algorithm is not as good as doing a global optimization across all maturities. If the data is wrong at some maturity, the following maturities might not calibrate. A global calibration would improve that problem, but might have other even worse problems. I guess that a jump in the term structure of volatility might not be captured by Heston model. For the very short term, the literature mentions that it is necessary to introduce jumps to fit market data."

Since almost all the calibrations succeed until at least 4y maturity, we now study the TS Heston parameters in the first five periods. We take out the two days on which calibration fails in Period 4 and another day on which the parameters have too dramatic changes compared with previous and later days. Hence, the total number of days in our plots is 255.

We show the plots of the correlation parameter in the first five periods in Figure 3. We can see that generally the correlation in the later periods is larger in magnitude compared to the previous ones. This corresponds well to the market data where the risk reversal is greater in magnitude on the later maturities. Also the correlation values in the different periods move approximately in the same direction, which is again correspondent to the market data in which the value of risk reversals in different periods increase or decrease in the same direction.

The range of the correlation is around 0.25 in the first three periods: -0.2 to 0.05 in period 1, -0.22 to 0.02 in period 2, and -0.25 to 0 in period 3. In period 4 and period 5, the ranges become much wider: -0.6 to 0.1 in the former and -0.5 to 0.1 in the latter. Hence we can expect even wider range in the later periods which finally drives the correlation into -1 and results in the calibration failure. This is indeed the case in the next two periods where the calibration breaks down on 201 of the 258 days (77.91%).

In Figure 4, we show the values of the mean reversion level in different periods. We can see that the mean reversion level in period 2 (6m - 1y) is generally the largest. When we check the market data, we find that the At-the-Money volatility at the 1y maturity is on most of the days higher than those of the other maturities and that the volatility surface has a downward slope after that.

When we look at the mean reversion level in each period respectively, we observe the phenomenon of volatility clustering in almost all the periods. Take the first sub-figure as an example. The mean reversion level first fluctuates around a small value. Then on a certain day it jumps to a larger value and fluctuates around that for an number of days, which is followed by another jump to an even larger value. This suggests that the market changes the view at least twice on the future long term volatility level.

Finally we plot the volatility of variance (vol of vol) in Figure 5. From the sub-figures, it seems that vol of vol fluctuates around a certain mean value. When we check the market data, we find that the value of the strangles also fluctuates around a certain mean value. This is in agreement with the relationship between strangle and vol of vol.

In conclusion, we find that when the market data (ATM, RR or STR) change greatly with the passage of time, the corresponding Heston parameters will also experience quite large changes. Hence, we can only expect stable parameters when the market data remain stable. Changing model parameters therefore requires us to take extra effort in hedging.

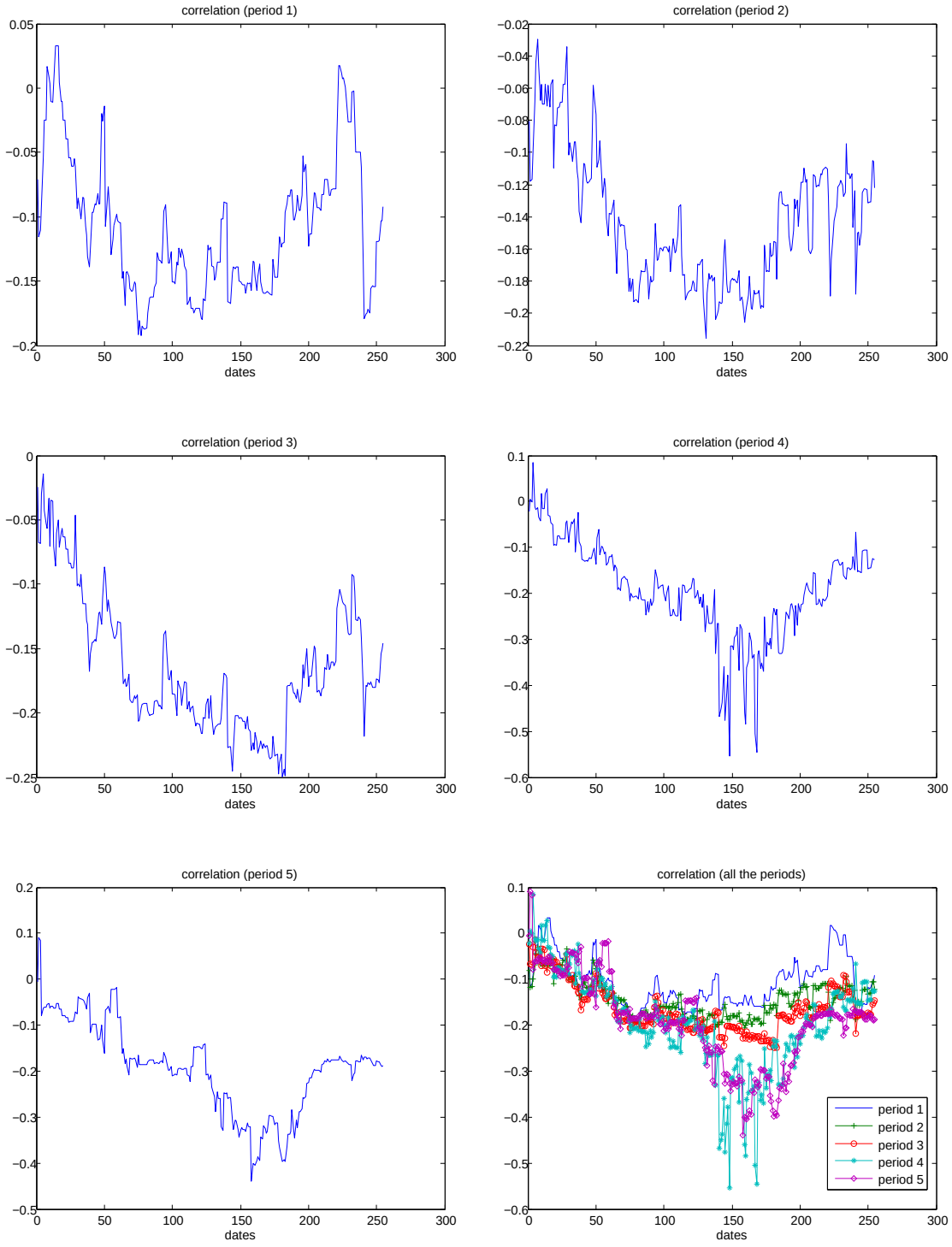

Figure 3: Term structure parameters: correlation, calibrated to the EUR/USD historic market data from Sep. 3, 2007 to Aug. 29, 2008

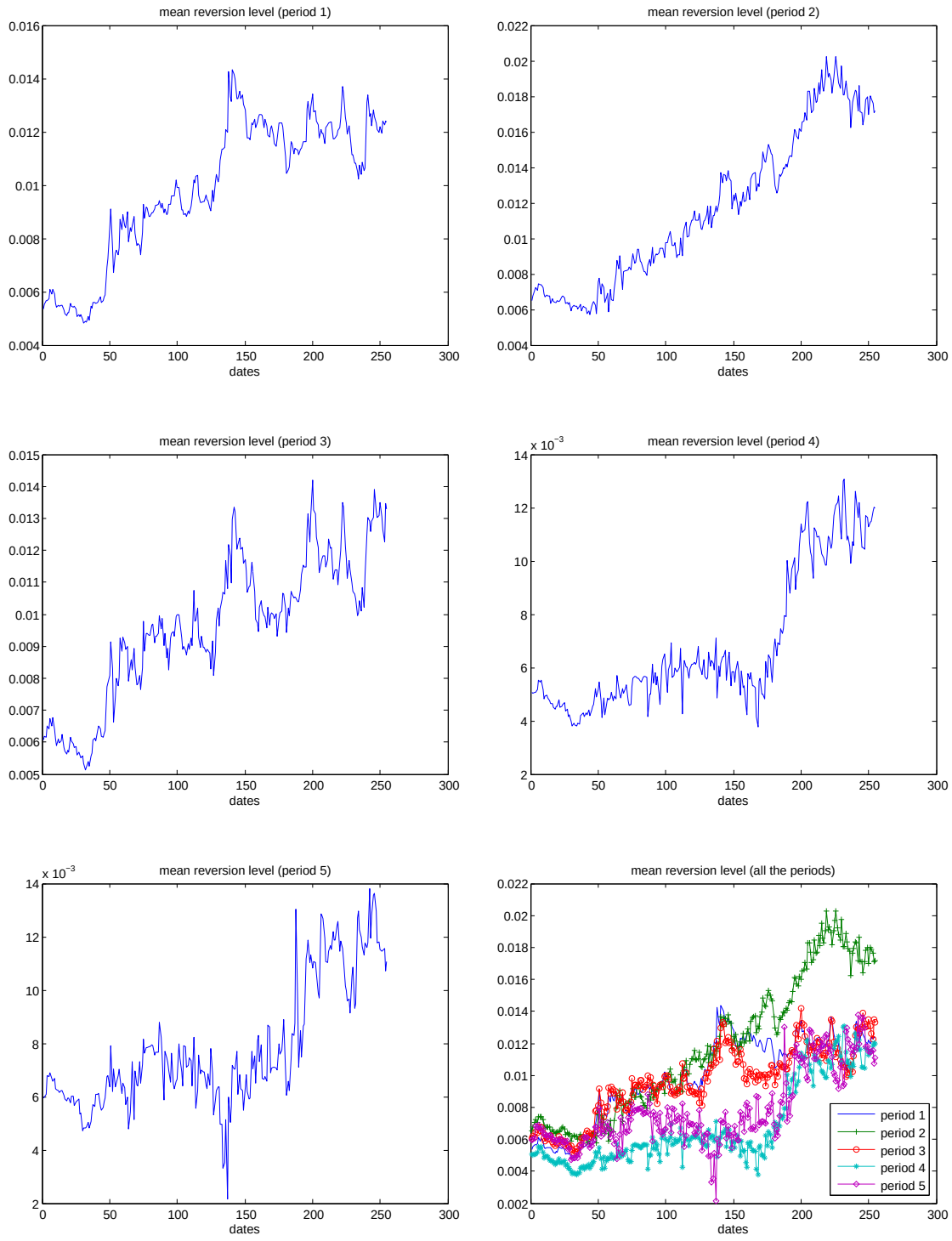

Figure 4: Term structure parameters: mean reversion level, calibrated to the EUR/USD historic market data from Sep. 3, 2007 to Aug. 29, 2008

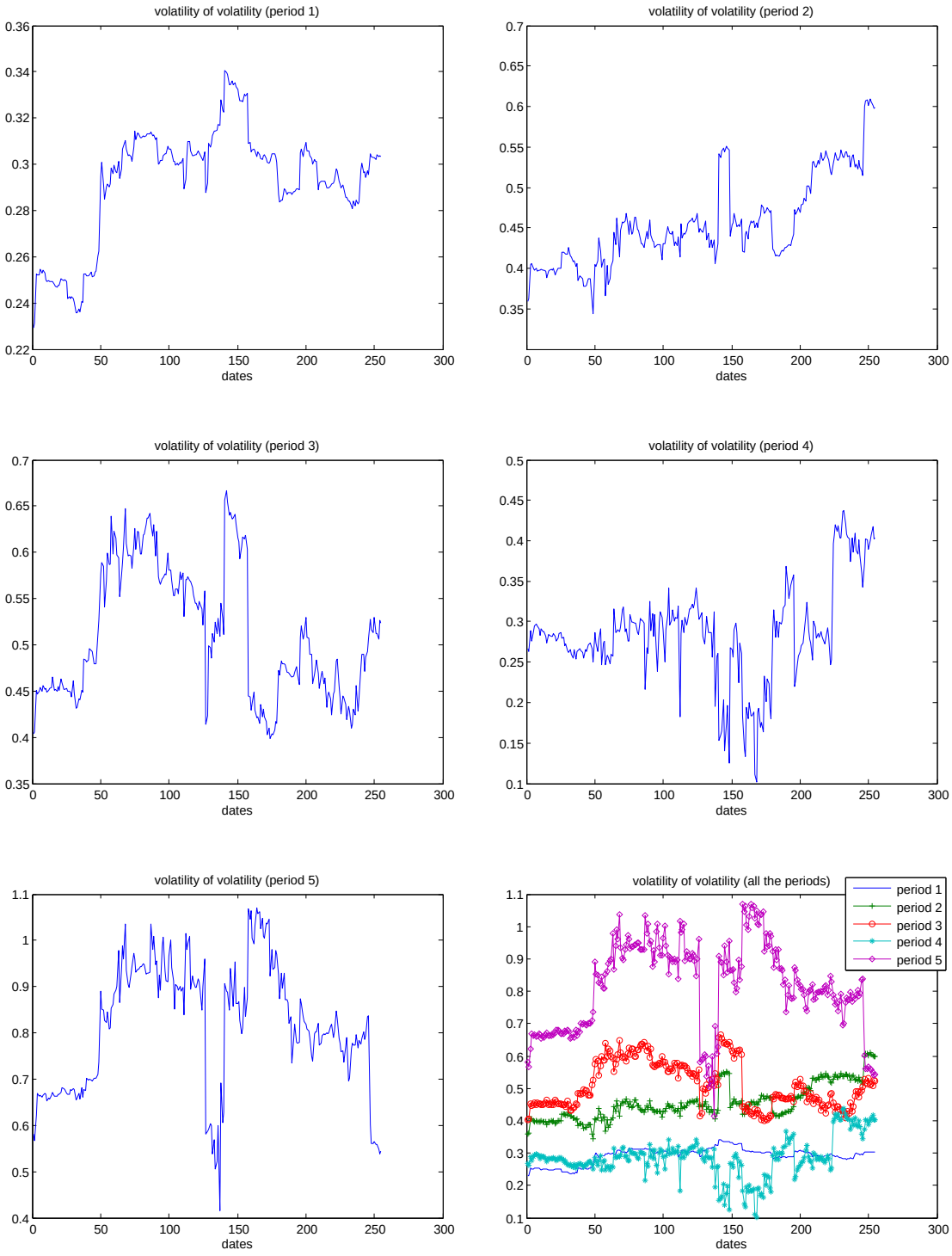

Figure 5: Term structure parameters: volatility of variance, calibrated to the EUR/USD historic market data from Sep. 3, 2007 to Aug. 29, 2008

8 Pricing exotic options

8.1 Exotic options in the FX market

8.1.1 Barrier options

In the FX market, there are many exotic options in addition to the vanilla options. The most popular one is the barrier option. A barrier option is a type of option whose payoff not only depends on the spot at the maturity, but on the underlying's crossing or reaching a given barrier level as well. They can either be call or put, and American or European. "In" options start their lives worthless and only become active when the knock-in barrier level is breached. "Out" options start their lives active and become valueless when the knock-out barrier level is breached. Using barrier options, the buyers can keep the premium at a lower level if they are sure that the spot movement will be limited within a certain range.

The popularity of barrier options is due to the following reasons [7]:

1. They are cheaper than the vanilla options: the closer the spot is to the barrier, the cheaper the knock-out option. Any price between zero and the vanilla premium can be obtained by taking an appropriate barrier level. However, one must be aware that too cheap barrier options are very likely to knock out and become valueless.

2. They allow FX risk exposure to be designed to meet special needs of customers. Instead of lowering the premium, one can increase the nominal coverage of the vanilla option by admitting a barrier. Some customers feel sure about barrier levels not being hit before the maturity of the option and could exploit to lower the premium. Others could require a knock-in option if they only want to cover their exchange rate exposure if the market moves drastically.

3. The money saved on the lower premium can be used for another hedge of FX risk exposure if the first barrier option happens to knock out.

4. The contract is easy to understand if one knows about vanillas.

5. Pricing and hedging barriers in the Black-Scholes model are well-understood and closed-form solutions are available.

There are four main types of barrier options:

1. Up-and-out: spot starts below the barrier level and has to move up for the option to be knocked out.

2. Down-and-out: spot starts above the barrier level and has to move down for the option to be knocked out.

3. Up-and-in: spot starts below the barrier level and has to move up for the option to become activated.

4. Down-and-in: spot starts above the barrier level and has to move down for the option to become activated.

In the Black-Scholes model, the analytic formula for pricing the barrier options exist [11]. Suppose H is the barrier level and K is the strike.

When the barrier level is lower than or equal to the strike, and the initial FX spot is higher than the barrier level:

$$C_{down-in} = S_0 e^{-r_f T}\left(\frac{H}{S_0}\right)^{2m} N(y) - K e^{-r_d T}\left(\frac{H}{S_0}\right)^{2m-2} N(y-\sigma\sqrt{T}) \quad (78)$$

$$\begin{aligned} P_{down-in} &= -S_0 e^{-r_f T} N(-x_1) + K e^{-r_d T} N(-x_1+\sigma\sqrt{T}) + S_0 e^{-r_f T}\left(\frac{H}{S_0}\right)^{2m}(N(y)-N(y_1)) \\ &\quad -K e^{-r_d T}\left(\frac{H}{S_0}\right)^{2m-2}[N(y-\sigma\sqrt{T}) - N(y_1-\sigma\sqrt{T})] \end{aligned} \quad (79)$$

When the barrier level is lower than or equal to the strike, and the initial FX spot is lower than the barrier level:

$$C_{up-in} = C_{BS} \quad (80)$$

$$\begin{aligned} P_{up-out} &= -S_0 e^{-r_f T} N(-x_1) + K e^{-r_d T} N(-x_1+\sigma\sqrt{T}) + S_0 e^{-r_f T}\left(\frac{H}{S_0}\right)^{2m} N(-y_1) \\ &\quad -K e^{-r_d T}\left(\frac{H}{S_0}\right)^{2m-2} N(-y_1+\sigma\sqrt{T}) \end{aligned} \quad (81)$$

When the barrier level is greater than the strike, and the initial FX spot is higher than the barrier level:

$$\begin{aligned} C_{down-out} &= S_0 e^{-r_f T} N(x_1) - K e^{-r_d T} N(x_1-\sigma\sqrt{T}) - S e^{-r_f T}\left(\frac{H}{S_0}\right)^{2m} N(y_1) \\ &\quad -K e^{-r_d T}\left(\frac{H}{S_0}\right)^{2m-2} N(y_1-\sigma\sqrt{T}) \end{aligned} \quad (82)$$

$$P_{down-in} = P_{BS} \quad (83)$$

When the barrier level is greater than the strike, and the initial FX spot is lower than the barrier level:

$$\begin{aligned} C_{up-in} &= S_0 e^{-r_f T} N(x_1) - K e^{-r_d T} N(x_1-\sigma\sqrt{T}) - S_0 e^{-r_f T}\left(\frac{H}{S_0}\right)^{2m}(N(-y)-N(-y_1)) \\ &\quad +K e^{-r_d T}\left(\frac{H}{S_0}\right)^{2m-2}[N(-y+\sigma\sqrt{T}) - N(-y_1+\sigma\sqrt{T})] \end{aligned} \quad (84)$$

$$P_{up-in} = -S_0 e^{-r_f T}\left(\frac{H}{S_0}\right)^{2m} N(-y) + K e^{-r_d T}\left(\frac{H}{S_0}\right)^{2m-2} N(y+\sigma\sqrt{T}) \quad (85)$$

where

$$y = \frac{ln(H^2/S_0K)}{\sigma\sqrt{T}} + m\sigma\sqrt{T} \tag{86}$$

$$m = \frac{r_d - r_f + 0.5\sigma^2}{\sigma^2} \tag{87}$$

$$x_1 = \frac{ln(S_0/H)}{\sigma\sqrt{T}} + m\sigma\sqrt{T} \tag{88}$$

$$y_1 = \frac{ln(H/S_0)}{\sigma\sqrt{T}} + m\sigma\sqrt{T} \tag{89}$$

$r_{d/f}$ is continuously compounded zero rate for the domestic/foreign currency corresponding to the maturity of the option, σ is the volatility, S_0 is the initial FX spot, T is the time to the maturity, and $N(x)$ is the cumulative normal distribution of x.

The prices of the other barrier options can be calculated according to the "in-out parity":

$$C_{BS} = C_{down-out} + C_{down-in} \tag{90}$$

$$C_{BS} = C_{up-out} + C_{up-in} \tag{91}$$

$$P_{BS} = P_{down-out} + P_{down-in} \tag{92}$$

$$P_{BS} = P_{up-out} + P_{up-in} \tag{93}$$

8.1.2 Double barrier options

One variation of the barrier option is the double barrier option. A double barrier option has two barriers, one above and the other below the current spot price. The payoff depends on whether the up-barrier or down-barrier is hit, or no breaching of either barrier throughout the whole life of the option. A barrier is said to be of knock-out type if the resulting payoff when hit is a rebate payment (the rebate amount may depend on the time of hitting and can be zero), and knock-in type if the holder receives a new option (call or put) upon hitting. The barrier feature may be applied over the whole life or a partial life of the option. A great number of double barrier options can be designed to achieve a wide variety of risk management functions through various structures. Like single barrier options, an investor buying a double barrier option may use the more exotic forms of the double barrier feature to achieve reduction in option premium, match investor's belief about the future movement of the stock price process and/or match his specific hedging needs more [12].

In the Black-Scholes model, double barrier options also admit closed-form solutions (we assume no rebate here) [13]. Suppose the payoff, $(\widetilde{a}+\widetilde{b}S)$, is a linear function of the underlying price S inside the interval $[X_1, X_2]$ and zero elsewhere.

Define the following parameter set

$$\Lambda = (\widetilde{a}, \widetilde{b}, X_1, X_2, r_d, r_f, \sigma, T) \tag{94}$$

where $r_{d/f}$ is continuously compounded zero rate for the domestic/foreign currency corresponding to the maturity of the option, σ is the volatility and T is the time to the maturity.

The value of the option is

$$V(S_0, \Lambda) = \widetilde{a}e^{-r_d T}[N(d_2^{X_1}) - N(d_2^{X_2})] + \widetilde{b}S_0 e^{-r_f T}[N(d_1^{X_1}) - N(d_1^{X_2})] \tag{95}$$

where

$$d_1^{(K)} = \frac{log(S_0/K) + (r_d - r_f)T}{\sigma\sqrt{T}} + \frac{\sigma\sqrt{T}}{2} \tag{96}$$

$$d_2^{(K)} = d_1^{(K)} - \sigma\sqrt{T} \tag{97}$$

and $K \in [X_1, X_2]$.

Standard call and put options can be regarded as special cases. Setting $X_1 = K$, $X_2 = \infty$, $\widetilde{a} = -K$ and $\widetilde{b} = 1$ gives the price of a standard call option with strike K:

$$C_{BS}(S_0, X, r_d, r_f, \sigma, T) = S_0 e^{-r_f T} N(d_1) - K e^{-r_d T} N(d_2) \tag{98}$$

Similarly, setting $X_1 = 0$, $X_2 = K$, $\widetilde{a} = K$ and $\widetilde{b} = -1$ yields the price of a standard put option with strike K:

$$P_{BS}(S_0, X, r_d, r_f, \sigma, T) = K e^{-r_d T} N(-d_2) - S_0 e^{-r_f T} N(-d_1) \tag{99}$$

8.1.3 Discrete barrier options

For a discrete barrier option, whether the barrier is breached or not is checked at discrete times (barrier dates). In practice most, if not all, barrier options traded in markets are discretely monitored. In other words, they specify fixed times for monitoring of the barrier (typically daily closings). Besides practical implementation issues, there are some legal and financial reasons why discretely monitored barrier options are preferred to continuously monitored barrier options. For example, some discussions in traders literature [22] pose the concern that, when the monitoring is continuous, extraneous barrier breach may occur in less liquid markets while the major western markets are closed, and may lead to certain arbitrage opportunities [14].

8.1.4 Parisian options

A Parisian option is a barrier option where the barrier condition applies only when the price of the underlying instrument has spent at least a given period of time on the "wrong" side of the barrier. Hence, Parisian options are essentially a crossover between barrier options and Asian options. They are similar to barrier option features in that they can be knocked in or out depending on hitting a barrier from under or above; they differ from standard barrier

options in that short-lived spot spikes will not trigger the Parisian, and for the trigger to be activated or extinguished, the asset must lie outside or inside the barrier for a predetermined time period, t [17].

There are two different kinds of Parisian options, cumulative and standard. For a cumulative Parisian option, the payoff is dependent on the total amount of time the underlying asset value has spent above or below a barrier level; for a standard Parisian option, the payoff is dependent on the maximum amount of time the underlying asset value has spent consecutively above or below a barrier level. Hence, all other parameters being equal, the standard Parisian option is usually cheaper than the cumulative Parisian option.

For discrete Parisian options, the payoff does not depend on the total amount of time but on the total number of barrier dates on which the underlying asset is above or below a barrier level, and for the trigger to be activated or extinguished, the number must exceed the maximum number of knocks, n. Thus, for a cumulative discrete Parisian option, the payoff is dependent on the number of the longest sequence of consecutive barrier dates on which the underlying asset value is above or below a barrier level; for a standard discrete Parisian option, the payoff is dependent on the total number of barrier dates on which the underlying asset value is above or below a barrier level. Similarly, all other parameters being equal, the Standard Discrete Parisian option is usually cheaper than the Cumulative Discrete Parisian option.

The discrete barrier option is a special case of the discrete Parisian option. When the maximum number of knocks is equal to one, the discrete Parisian option becomes the discrete barrier option. Hence, all other parameters being equal, the discrete Parisian option is usually cheaper than the discrete barrier option.

8.2 Pricing exotic options using Monte Carlo

For discretely monitored options, closed-form solutions exist in some models. For example, [15] applied the COS method on the discrete barrier options in the Black-Scholes, NIG (the Normal Inverse Gaussian Lévy process) and CGMY [23] models. However, in the Heston model, very few papers present the analytic solutions. One of them is [16]. They derive multivariate characteristic functions depending on at least two spot values for different points in time. The derived characteristic functions are used as building blocks to set up (semi-) analytical pricing formulas for exotic options with payoffs depending on finitely many spot values such as fader options and discretely monitored barrier options. This approach, although feasible, is computationally quite complex.

We have tried to apply the COS method to the discretely monitored options in the Heston model, but have not succeeded yet. The pricing results still have quite large errors. We put our current results in Section 9 as a future research direction.

Hence, we still use the Monte Carlo simulation to price barrier options, but we propose some new control variates which can significanlty reduce the variance. The pricing results are

shown and compared in 8.5, which include results in ordinary Heston model and TS Heston model, with control variates and without control variates.

8.3 Applying control variates for variance reduction in MC

In Monte Carlo simulation, variance reduction techniques are employed to increase the precision of the result, reduce the number of iterations needed to obtain a certain confidence interval and save simulation time. The main variance reduction techniques used are common random numbers, antithetic sampling, control variates, importance sampling and stratified sampling.

Control variates can be applied when we want to price an option and have an accurate price (usually analytic formula) for another option, usually a highly correlated one.

8.3.1 Basic principles of control variates

Suppose we want to value an option Y, the price estimate given by Monte Carlo simulation is

$$M = E[Y] \tag{100}$$

Suppose further that we have another option and its price process V is also driven by the same random variables. It has mean value $\mu_v = E[V]$. Then instead of using Y as an estimate for the original option we want to price, we replace it with

$$W = Y + c(V - \mu_v) \tag{101}$$

where c is a constant to be specified so as to achieve the maximum reduction of variance. Since $E[W] = E[Y] = M$, W is an unbiased estimate of Y and its variance is given by

$$Var(W) = Var(Y) + c^2 Var(V) + 2cCov(Y, V) \tag{102}$$

where $Cov(Y, V)$ is the covariance between Y and V.

Thus, in order to minimize $Var(W)$, we set

$$c = -\frac{Cov(Y, V)}{Var(V)} \tag{103}$$

Substitute this back into (102), we have

$$Var(W) = Var(Y) - Cov^2(Y, V)/Var(V) \tag{104}$$

That is,

$$\frac{Var(W)}{Var(Y)} = 1 - Corr^2(Y, V) \tag{105}$$

where $Corr(Y, V)$ is the correlation between Y and V.

Hence, the higher the correlation between the two options, the greater the variance reduction can be achieved.

8.3.2 Using multiple control variates

Sometimes, using multiple control variates can further reduce the variance. Suppose V is a combination of several options,

$$V = \sum_{i=1}^{n} \alpha_i V_i \tag{106}$$

where α_i are weights to be determined so as to achieve the maximum reduction of variance. According to equation (101), the estimate of Y reads

$$W = Y + (V - E[V]) \tag{107}$$

We have

$$Var(W) = Var(Y) + \sum_{i=1}^{n} \alpha_i^2 Var(V_i) + \sum_{i=1}^{n} 2\alpha_i Cov(Y, V_i) + \sum_{i=1}^{n} \sum_{j=1, i\neq j}^{n} 2\alpha_i \alpha_j Cov(V_i, V_j) \tag{108}$$

Writing in matrix form, we have

$$Var(W) = Var(Y) + \alpha^T \mathbf{A} \alpha + 2\beta^T \alpha \tag{109}$$

where

$$\alpha = (\alpha_1, \alpha_2, ..., \alpha_n)^T \tag{110}$$

$$\mathbf{A} = \begin{bmatrix} Var(V_1) & Cov(V_1, V_2) & ... & Cov(V_1, V_n) \\ Cov(V_1, V_2) & Var(V_2) & ... & Cov(V_2, V_n) \\ \vdots & & \ddots & \vdots \\ Cov(V_1, V_n) & \dots & & Var(V_n) \end{bmatrix} \tag{111}$$

and

$$\beta = (Cov(Y, V_1), Cov(Y, V_2), ..., Cov(Y, V_n))^T \tag{112}$$

Note that $\mathbf{A}$ is a symmetric matrix.

According to the matrix calculus, suppose that $\mathbf{f}(x)$ and $\mathbf{g}(x)$ are two vectors, we have

$$\frac{d(\mathbf{f}(x)^T \mathbf{g}(x))}{dx} = \mathbf{g}(x)^T \mathbf{f}'(x) + \mathbf{f}(x)^T \mathbf{g}'(x) \tag{113}$$

Hence, applying it to $\alpha^T \mathbf{A} \alpha$, we have

$$\frac{d(\alpha^T \mathbf{A} \alpha)}{d\alpha} = \alpha^T \mathbf{A} + \alpha^T \mathbf{A}^T = \alpha^T (\mathbf{A} + \mathbf{A}^T) \tag{114}$$

Since $\mathbf{A}$ is a symmetric matrix, we have

$$\frac{d(\alpha^T \mathbf{A} \alpha)}{d\alpha} = 2\alpha^T \mathbf{A} \tag{115}$$

To minimize the variance, we have

$$\begin{aligned} 2\alpha^T \mathbf{A} + 2\beta^T &= 0 \\ \alpha^T \mathbf{A} &= -\beta^T \\ \mathbf{A}^T \alpha &= -\beta \\ \alpha &= -\mathbf{A}^{-1}\beta \end{aligned} \tag{116}$$

Substitute this back into (109), we have

$$Var(W) = Var(Y) - \beta^T A^{-1} \beta \tag{117}$$

That is

$$\frac{Var(W)}{Var(Y)} = 1 - \beta^T A^{-1} \beta / Var(Y) \tag{118}$$

Equating it with equation (105), we obviously have

$$Corr^2(Y, V) = \beta^T \mathbf{A}^{-1} \beta / Var(Y) \tag{119}$$

When the correlations between the V_i are very low, $\mathbf{A}$ is close to a diagonal matrix. Then

$$\alpha_i = -\frac{Cov(Y, V_i)}{Var(V_i)} \tag{120}$$

Substitute this back into (109), we have

$$Var(W) = Var(Y) - \sum_{i=1}^{n} \frac{Cov(Y, V_i)^2}{Var(V_i)} \tag{121}$$

That is,

$$\frac{Var(W)}{Var(Y)} = 1 - \sum_{i=1}^{n} Corr^2(Y, V_i) \tag{122}$$

Since we want to choose options which have high correlations with the option we want to price as control variates, they usually have high correlations with each other. Hence we normally cannot simplify (116) to (120) as in [10].

8.4 Pricing discrete barrier options using Monte Carlo with control variates

We now use the control variates for the Monte Carlo simulation to price the discrete barrier option. The critical issue is to find another option as a control variate which has the highest correlation with the discrete barrier option and can be priced analytically as well.

Chu [18] proposed several control variates for the discrete barrier option in the BS model:

1. Continuously monitored barrier options with the same barriers and the same strike

The difference between the continuous barrier and discrete barrier is the observation frequency. The continuously-monitored barrier option becomes valueless, as soon as the price of the underlying asset reaches the barrier level during the life of the option. Hence, theoretically the price of the continuously-monitored barrier option is the lower bound for the price of the discretely-monitored barrier option. As the number of observed dates increases, their prices become much closer. Thus, the continuously-monitored barrier option is a better control variate for the discretely-monitored barrier option when the number of observation dates is large.

2. Portfolio of standard European options

Derman, Ergener and Kani [19] proposed the static options replication technique which involves searching for a portfolio of standard European options that approximately replicate the boundary condition satisfied by the barrier option. The basic principle is that two portfolios are worth the same at all interior points of the boundary if they are worth the same on a certain boundary. Suppose T, K and B are the maturity, strike and barrier levels of a discrete barrier option respectively and $C(T,K)$ is a vanilla option with maturity T and strike K. The portfolio could be only $C(T,K)$, or $C(T,K)$ and $C(T,B)$, or $C(T,K)$ and $C(T_i,B)$, where T_i are the specified dates until maturity.

Chu [18] shows that continuously monitored barrier options perform much better than portfolios of standard European options. However, we hardly find any analytic solution for the continuous barrier option in the Heston model. Therefore, instead of using continuous barrier options, we choose different portfolios of European barrier options and European options as control variates.

For a European barrier option, the barrier only exists at the maturity. Hence we can use the COS method to price it. Suppose K is the strike, Rb is the rebate, L the lower barrier and H the higher barrier of the discrete barrier options respectively. The payoff function for a European double barrier option reads

$$\begin{aligned} v(y,T) &= \{\max(\alpha(S_T-K),0)-Rb\}\mathbf{1}_{\{L<S_T<H\}}+Rb \\ &= \{[\alpha\cdot K(e^y-1)]^+-Rb\}\mathbf{1}_{\{h_{down}<y<h_{up}\}}+Rb \end{aligned} \tag{123}$$

where $\alpha=1$ for a call, $\alpha=-1$ for a put, $y=log(S_T/K)$, $h_{down}=log(L/K)$ and $h_{up}=log(H/K)$.

Define the cosine series coefficients, χ_k, of $g(y)=e^y$ on $[c,d]\subset[a,b]$ which is known analytically as shown in equation (22) in [3]:

$$\begin{aligned} \chi_k(c,d) &:= \int_c^d e^y cos\left(k\pi\frac{y-a}{b-a}\right)dy \\ &= \frac{1}{1+\left(\frac{k\pi}{b-a}\right)^2}\left[cos\left(k\pi\frac{d-a}{b-a}\right)e^d-cos\left(k\pi\frac{c-a}{b-a}\right)e^c\right. \\ &\quad \left.\frac{k\pi}{b-a}sin\left(k\pi\frac{d-a}{b-a}\right)e^d-\frac{k\pi}{b-a}sin\left(k\pi\frac{c-a}{b-a}\right)e^c\right] \end{aligned} \tag{124}$$

and the cosine series coefficients, ψ_k, of $g(y) = 1$ on $[c,d] \subset [a,b]$ which is also known analytically as shown in equation (23) in [3]:

$$\begin{aligned}\psi_k(c,d) &:= \int_c^d cos\left(k\pi\frac{y-a}{b-a}\right)dy \\ &= \begin{cases} \left[sin\left(k\pi\frac{d-a}{b-a}\right) - sin\left(k\pi\frac{c-a}{b-a}\right)\right]\frac{b-a}{k\pi} & k \neq 0 \\ d-c & k = 0 \end{cases}\end{aligned} \tag{125}$$

Hence, according to the definition of V_k in (37), we have

$$V_k = \frac{2}{b-a}\alpha K\left[\chi_k(x_1,x_2) - \psi_k(x_1,x_2)\right] + \frac{2}{b-a}Rb\left[\psi_k(a,x_3) + \psi_k(x_4,b)\right] \tag{126}$$

where $x_1 = \max\{a, h_{down}, 0\}$, $x_2 = \min\{b, h_{up}\}$ for a call, and $x_1 = \max\{a, h_{down}\}$, $x_2 = \min\{b, h_{up}, 0\}$ for a put. For both call and put, $x_3 = \max\{a, h_{down}\}$ and $x_4 = \min\{b, h_{up}\}$.

Substitute (126) into (40) to get the semi-analytic value for the European barrier option. This paves the way to use European barrier options as control variates.

Suppose that T_i^B are the barrier dates and T is the maturity date. Further suppose that $C^B(T,K,L,H)$ ($P^B(T,K,L,H)$) and $C(T,K)$ ($P(T,K)$) are European barrier call (put) option and European call (put) option respectively. The control variates portfolios we try for the discrete barrier call options are:

1. $C^B(T,K,L,H)$
2. $C^B(T,K,L,H)$ and $C^B(T_i^B,K,L,H)$
3. $C^B(T,K,L,H)$, $C(T_i^B,H)$ and $P(T_i^B,L)$
4. $C^B(T,K,L,H)$, $C(T_i^B,L)$ and $P(T_i^B,H)$
5. $C^B(T,K,L,H)$ and $C(T_i^B,K)$
6. $C^B(T,K,L,H)$, $C(T_i^B,K)$ and $P(T_i^B,K)$
7. $C^B(T,K,L,H)$, $C^B(T_i^B,K,L,H)$ and $P^B(T_i^B,K,L,H)$

We have found in the tests that by using European barrier option $C^B(T,K,L,H)$ alone, the variance is already greatly reduced (between 6% and 66% depending on the options and market data). By including more options, either European barrier options or European options, we can further reduce the variance by a small percentage, but this involves calculating the variance and covariance between all the control variants and the discrete barrier option.

In the tests, we have also found that the mean values of the control variate deviate from their analytic values for some options (even when the number of paths is very large), which makes the MC simulation results with CV differ from those without. Theoretically, by the law of large numbers, this method will display $1/\sqrt{N}$ convergence. The difference suggests certain problem in the MC simulation, and we think it might be the negative volatility caused by the Euler discretization when the Feller condition does not satisfy (which is often the case). For example, for a 5-year option, the fraction of negative volatility could be as high as nearly 40%. Hence, by including the CV, we think we could not only reduce the variance, but eliminate the bias in the expectation of the MC simulation result as well.

In all the tests, the parameters we use are the ones calibrated to the market data shown in table 38. The mean reversion rate, κ, is set to 2 in all the cases. The variance reduction achieved is calculated by

$$\frac{\text{Var with CV} - \text{Var without CV}}{\text{Var without CV}} \times 100\% \tag{127}$$

We first test on the one-year discrete (double) barrier call options with different strikes, both with term structure and without term structure. The number of barrier dates is set to 24 (set on the 2nd and 9th day of each month). From Table 14 and Table 15, we can see that using a European barrier option with one-year maturity (Portfolio 1) alone has already greatly reduce the variance, on average by 43.34% in the ordinary Heston and 42.41% in the TS Heston. By including more options with maturities on each barrier date, we can further reduce the variance, but only by a small percentage. We can see that from Portfolio 2 to Portfolio 7, Portfolio 2 (European barrier options with strike K on each barrier date) and Portfolio 7 (both European call and put options with strike K on each barrier date) achieve a slightly better variance reduction than the other 4 portfolios. However, by including more options in the control variates, the time to compute the mean and covariance matrix of the options also increases dramatically (on the order of N^2). It is not worth spending much time in order to achieve a slight improvement.

We can also see that when the barrier level becomes closer to the spot, the variance reduction also becomes smaller. This is because the closer the barrier level is to the spot, the higher the chance that the underlying will breach a barrier on one of the barrier dates but ends within the barriers at maturity. This greatly reduces the effect of control variates.

L	H	K	Portfolio 1	Portfolio 2	Portfolio 3	Portfolio 4	Portfolio 5	Portfolio 6	Portfolio 7
1	1.6	1.2	-65.54%	-68.18%	-66.49%	-66.99%	-67.08%	-67.74%	-68.31%
1	1.5	1.2	-49.73%	-53.41%	-51.67%	-52.92%	-53.05%	-54.16%	-53.46%
1	1.4	1.2	-22.53%	-27.29%	-25.44%	-29.30%	-29.29%	-30.51%	-27.65%
1.2	1.6	1.2	-58.41%	-62.46%	-59.54%	-59.72%	-59.02%	-59.42%	-62.46%
1.2	1.5	1.2	-44.58%	-50.39%	-46.40%	-46.62%	-45.55%	-46.30%	-50.39%
1.2	1.4	1.2	-19.26%	-26.24%	-21.64%	-23.17%	-34.39%	-23.82%	-26.24%
Average			-43.34%	-48.00%	-45.20%	-46.45%	-48.06%	-46.99%	-48.09%
Num of Options			1	24	48	48	24	48	48

Table 14: The percentage of variance reduction achieved using different control variates portfolios for discrete (double) barrier call options with 24 barrier dates (two per month) and 1-year maturity in (ordinary) Heston model. The spot FX is 1.3621.

Next we test on five-year discrete (double) barrier call options with different strikes, both with term structure and without term structure. The number of barrier dates is set to 5 (one barrier date per year). From Table 16 and Table 17, we can see again that using European barrier option with five-year maturity (Portfolio 1) alone has already greatly reduced the variance, by average 42.17% in ordinary Heston and 44.25% in TS Heston. Again, using

L	H	K	Portfolio 1	Portfolio 2	Portfolio 3	Portfolio 4	Portfolio 5	Portfolio 6	Portfolio 7
1	1.6	1.2	-65.33%	-67.05%	-66.81%	-67.44%	-67.17%	-67.91%	-67.20%
1	1.5	1.2	-48.90%	-51.44%	-50.86%	-52.47%	-52.49%	-53.73%	-51.50%
1	1.4	1.2	-21.06%	-25.74%	-24.02%	-27.88%	-27.69%	-27.69%	-26.15%
1.2	1.6	1.2	-58.03%	-61.55%	-59.64%	-59.51%	-58.53%	-59.02%	-61.55%
1.2	1.5	1.2	-43.39%	-48.20%	-45.25%	-45.52%	-44.35%	-45.25%	-48.20%
1.2	1.4	1.2	-17.78%	-24.90%	-20.16%	-21.50%	-21.05%	-17.73%	-24.90%
Average			-42.41%	-46.48%	-44.46%	-45.72%	-45.21%	-45.22%	-46.58%
Num of Options			1	24	48	48	24	48	48

Table 15: The percentage of variance reduction achieved using different control variates portfolios for discrete (double) barrier call options with 24 barrier dates (two per month) and 1-year maturity in TS Heston model. The spot FX is 1.3621.

the other portfolios can further reduce the variance, but only by a small percentage, where portfolio 2 (European barrier options with strike K on each barrier date) and portfolio 7 (both call and put options with strike K on each barrier date) perform slightly better.

We can see that the level of variance reduction in this case is similar to the previous case, although there are only five barrier dates (when there is only one, the variance reduction should be 100%). This shows that for options with long term maturities, the effect of control variates gradually reduces.

L	H	K	Portfolio 1	Portfolio 2	Portfolio 3	Portfolio 4	Portfolio 5	Portfolio 6	Portfolio 7
1	1.6	1.2	-63.02%	-64.76%	-63.56%	-64.14%	-64.51%	-65.07%	-64.92%
1	1.5	1.2	-50.04%	-52.06%	-50.87%	-51.74%	-52.23%	-52.83%	-52.55%
1	1.4	1.2	-31.61%	-33.83%	-32.52%	-33.42%	-33.80%	-34.16%	-34.79%
1.2	1.6	1.2	-51.15%	-55.88%	-51.70%	-51.75%	-51.35%	-51.69%	-55.88%
1.2	1.5	1.2	-37.56%	-43.45%	-38.25%	-38.37%	-38.03%	-38.46%	-43.45%
1.2	1.4	1.2	-19.62%	-25.50%	-20.18%	-20.37%	-20.24%	-20.52%	-25.50%
Average			-42.17%	-45.91%	-42.85%	-43.30%	-43.36%	-43.79%	-46.18%
Num of Options			1	5	10	10	5	10	10

Table 16: The percentage of variance reduction achieved using different control variates portfolios for discrete (double) barrier call options with 5 barrier dates (one per year) and 5-year maturity in (ordinary) Heston model. The spot FX is 1.3621.

Finally we test on five-year discrete (double) barrier call options with different strikes, both with term structure and without term structure. The number of barrier dates is set to 20 (one barrier date per 3 months). From Table 18 and Table 19, we can see again that most of the variance reduction is achieved by the European barrier option with five-year maturity (Portfolio 1), on average by 26.33% without term structure and by 27.54% with term structure. Again Portfolio 2 (European barrier options with strike K on each barrier date) and Portfolio 7 (both call and put options with strike K on each barrier date) perform

L	H	K	Portfolio 1	Portfolio 2	Portfolio 3	Portfolio 4	Portfolio 5	Portfolio 6	Portfolio 7
1	1.6	1.2	-63.83%	-65.77%	-64.40%	-64.93%	-65.23%	-65.83%	-65.90%
1	1.5	1.2	-51.91%	-54.18%	-52.83%	-53.88%	-54.98%	-54.34%	-54.65%
1	1.4	1.2	-34.93%	-37.43%	-35.96%	-37.26%	-37.44%	-37.84%	-38.44%
1.2	1.6	1.2	-53.97%	-58.90%	-54.59%	-54.63%	-54.18%	-54.63%	-58.90%
1.2	1.5	1.2	-40.26%	-46.44%	-41.07%	-41.23%	-40.88%	-41.43%	-46.44%
1.2	1.4	1.2	-20.60%	-27.42%	-21.29%	-21.37%	-21.18%	-21.57%	-27.42%
Average			-44.25%	-48.36%	-45.02%	-45.55%	-45.65%	-45.94%	-48.63%
Num of Options			1	5	10	10	5	10	10

Table 17: The percentage of variance reduction achieved using different control variates portfolios for discrete (double) barrier call options with 5 barrier dates (one per year) and 5-year maturity in TS Heston model. The spot FX is 1.3621.

L	H	K	Portfolio 1	Portfolio 2	Portfolio 3	Portfolio 4	Portfolio 5	Portfolio 6	Portfolio 7
1	1.6	1.2	-47.30%	-49.36%	-48.15%	-48.98%	-49.33%	-50.31%	-49.44%
1	1.5	1.2	-33.43%	-35.29%	-34.34%	-35.55%	-35.93%	-36.89%	-35.36%
1	1.4	1.2	-16.03%	-17.50%	-16.85%	-18.15%	-18.30%	-18.81%	-18.11%
1.2	1.6	1.2	-33.63%	-38.04%	-34.37%	-34.43%	-33.91%	-34.29%	-38.04%
1.2	1.5	1.2	-20.89%	-25.10%	-21.51%	-21.65%	-21.28%	-21.71%	-25.10%
1.2	1.4	1.2	-6.73%	-9.38%	-7.05%	-7.15%	-7.03%	-7.22%	-9.38%
Average			-26.33%	-29.11%	-27.05%	-27.65%	-27.63%	-28.21%	-29.24%
Num of Options			1	20	40	40	20	40	40

Table 18: The percentage of variance reduction achieved using different control variates portfolios for discrete (double) barrier call options with 20 barrier dates (one per 3 months) and 5-year maturity in (ordinary) Heston model. The spot FX is 1.3621.

L	H	K	Portfolio 1	Portfolio 2	Portfolio 3	Portfolio 4	Portfolio 5	Portfolio 6	Portfolio 7
1	1.6	1.2	-50.21%	-51.84%	-50.93%	-52.03%	-52.34%	-53.18%	-51.91%
1	1.5	1.2	-34.84%	-36.28%	-36.04%	-37.86%	-38.21%	-39.15%	-36.56%
1	1.4	1.2	-17.04%	-17.99%	-18.22%	-20.19%	-20.26%	-20.91%	-18.65%
1.2	1.6	1.2	-36.27%	-40.47%	-36.92%	-37.00%	-36.50%	-36.81%	-40.47%
1.2	1.5	1.2	-20.96%	-25.36%	-21.72%	-21.86%	-21.39%	-21.79%	-25.36%
1.2	1.4	1.2	-5.93%	-8.25%	-6.37%	-6.58%	-6.43%	-6.72%	-8.25%
Average			-27.54%	-30.03%	-28.37%	-29.25%	-29.19%	-29.76%	-30.20%
Num of Options			1	20	40	40	20	40	40

Table 19: The percentage of variance reduction achieved using different control variates portfolios for discrete (double) barrier call options with 20 barrier dates (one per 3 months) and 5-year maturity in TS Heston model. The spot FX is 1.3621.

slightly better than the other portfolios.

When the number of barrier dates is increased from 5 to 20, the amount of variance

reduction achieved is reduced. Hence for options with long maturities and many barrier dates, it is better to use other control variates (say continuous barrier options), but the problem then lies in the derivation of the analytic formula.

We also list the standard deviation in Table 20 to 22 as a reference. This can be used to calculate the confidence interval of our estimate.

L	H	K	Heston		TS Heston	
			std	std (with CV)	std	std (with CV)
1	1.6	1.2	0.106921	0.062768	0.107494	0.063297
1	1.5	1.2	0.084117	0.059638	0.082998	0.059328
1	1.4	1.2	0.040919	0.036016	0.039185	0.034815
1.2	1.6	1.2	0.108496	0.069970	0.108783	0.070475
1.2	1.5	1.2	0.083652	0.062277	0.082160	0.061818
1.2	1.4	1.2	0.038306	0.034419	0.036385	0.032993

Table 20: The standard deviation of Monte Carlo simulation with 10000 paths with and without CV for discrete (double) barrier call options with 24 barrier dates (two per month) and 1-year maturity in (ordinary) Heston and TS Heston model. The spot FX is 1.3621.

L	H	K	Heston		TS Heston	
			std	std (with CV)	std	std (with CV)
1	1.6	1.2	0.087622	0.053286	0.086606	0.052087
1	1.5	1.2	0.057920	0.040937	0.058044	0.040251
1	1.4	1.2	0.027803	0.022992	0.028619	0.023085
1.2	1.6	1.2	0.083193	0.058148	0.083348	0.056551
1.2	1.5	1.2	0.052359	0.041375	0.053198	0.041119
1.2	1.4	1.2	0.022393	0.020076	0.022658	0.020189

Table 21: The standard deviation of Monte Carlo simulation with 10000 paths with and without CV for discrete (double) barrier call options with 5 barrier dates (two per month) and 5-year maturity in (ordinary) Heston and TS Heston model. The spot FX is 1.3621.

In conclusion, we think that using European Barrier options with the same maturity as the original discrete barrier option can significantly reduce the variance, and we do not intend to include more options in the control variates. When the maturity of the option is short and the number of barrier dates is small, the effect of variance reduction is most significant.

L	H	K	Heston		TS Heston	
			std	std (with CV)	std	std (with CV)
1	1.6	1.2	0.078698	0.057132	0.080300	0.056662
1	1.5	1.2	0.049368	0.040278	0.050292	0.040596
1	1.4	1.2	0.020314	0.018615	0.021195	0.019305
1.2	1.6	1.2	0.070519	0.057450	0.072592	0.057949
1.2	1.5	1.2	0.040610	0.036120	0.040819	0.036289
1.2	1.4	1.2	0.013258	0.012804	0.012774	0.012390

Table 22: The standard deviation of Monte Carlo simulation with 10000 paths with and without CV for discrete (double) barrier call options with 20 barrier dates (one per 3 months) and 5-year maturity in (ordinary) Heston and TS Heston model. The spot FX is 1.3621.

8.5 Simulation results using Monte Carlo with control variates

Now we will show the simulation results both with and without control variates and then compare the prices given by the ordinary Heston model and the TS Heston model.

In all the tests, we still use the parameters calibrated to the market data shown in Table 38. The mean reversion rate, κ, is again set to 2 in all the cases. The relative error (rel. error) is calculated by

$$\text{Rel. Error} = \frac{C_{MC} - C_{ref}}{C_{ref}} \times 100\% \tag{128}$$

where C_{MC} is the MC simulation price of the option and C_{ref} is its reference value, either the analytic one or the MC simulation result with a significant number of paths.

In the tests, we find that there are some discrepancy between the results given by MC simulation with control variates and those without. Since the differences can only come from the control variates we have added, we first check their prices.

In Table 23 to 26, we can see that the MC simulation converges very slowly. For 1y European barrier options in TS Heston model (Table 24), the price seems not to converge at all. We suspect that it is because there is dramatic changes in the parameters and the Feller condition does not satisfy. Hence, we try to price the same European barrier options, but with smaller volatility of variance.

In Table 27, we show the simulation results of 1y European barrier options in TS Heston model with vol of vol parameters reduced by 50%. Although only the parameters of the first two periods (0-6m and 6m-9m) satisfy the Feller condition now, the fraction of negative volatility has already be greatly reduced from 0.179256 to 0.049603. The MC simulation results now converge to the analytic prices.

For the other cases where the MC simulation results converge, changing the parameters to make them Feller condition complied does not make much difference in the convergence.

Therefore, in certain cases where there are discrepancies between MC simulation results

L	H	K	Num of MC paths	price	relative error
1	1.6	1.2	10000	0.122652	0.98%
			400000	0.121596	0.11%
			analytical	0.121458	
1	1.5	1.2	10000	0.0896013	1.61%
			400000	0.0881844	0.00%
			analytical	0.0881824	
1	1.4	1.2	10000	0.0445847	1.83%
			400000	0.0436045	-0.41%
			analytical	0.043782	

Table 23: The MC price and analytic price of 1y European barrier call options in (ordinary) Heston model. The fraction of negative volatility in the simulation paths is 0.117607.

L	H	K	Num of MC paths	price	relative error
1	1.6	1.2	10000	0.121035	-0.36%
			400000	0.120582	-0.73%
			analytical	0.121474	
1	1.5	1.2	10000	0.0869643	-1.40%
			400000	0.0868087	-1.58%
			analytical	0.0882015	
1	1.4	1.2	10000	0.0431554	-1.36%
			400000	0.0428222	-2.12%
			analytical	0.0437519	

Table 24: The MC price and analytic price of 1y European barrier call options in TS Heston model. The fraction of negative volatility in the simulation paths is 0.179256.

and analytic values (say when the parameters undergo great changes from one period to another), using control variates not only reduces the variance of the simulation results, but somehow eliminates their biases as well.

Now we show the pricing results. As we have mentioned before, there are quite large differences between the simulation results with and without CV for discrete (double) barrier call options with 24 barrier dates (two per month) and 1-year maturity in TS Heston model, even if the number of paths is set to 400000 (see Table 29). This is due to the simulation errors in the CV, which we think should also exist in the simluation of the original Barrier options. Hence, we think that the MC results with CV are closer to the accurate results since the CV help to eliminate the biases.

We calculate the relative errors by taking the MC results of 400000 paths without CV

L	H	K	Num of MC paths	price	relative error
1	1.6	1.2	10000	0.0547018	1.79%
			400000	0.0538528	0.21%
			analytical	0.053738	
1	1.5	1.2	10000	0.0409117	-1.03%
			400000	0.0413376	0.00%
			analytical	0.0413358	
1	1.4	1.2	10000	0.0196083	-0.96%
			400000	0.0197339	-0.33%
			analytical	0.0197988	

Table 25: The MC price and analytic price of 5y European barrier call options in (ordinary) Heston model. The fraction of negative volatility in the simulation paths is 0.348872.

L	H	K	Num of MC paths	price	relative error
1	1.6	1.2	10000	0.0646294	-0.69%
			400000	0.0649998	-0.12%
			analytical	0.0650767	
1	1.5	1.2	10000	0.0412277	-0.14%
			400000	0.0411992	-0.21%
			analytical	0.0412868	
1	1.4	1.2	10000	0.0200192	1.24%
			400000	0.0197585	-0.08%
			analytical	0.0197747	

Table 26: The MC price and analytic price of 5y European barrier call options in TS Heston model. The fraction of negative volatility in the simulation paths is 0.394043.

as reference values. In Table 28 to 33, we see that all the simulation results without CV converges, but at a very slow rate. The number of paths need to be set to at least 50000 to get an accurate enough result. For the simulation results with CV, they do not always converge to the reference values we take, sometimes with relative errors of around 1%. But we think they give more accurate results.

One problem we find is that using CV sometimes slows the convergence of simulation result, especially in the (ordinary) Heston model. For example, for discrete (double) barrier call options with 24 barrier dates and 1-year maturity in Table 28, the differences between results with 50000 paths and 400000 paths for MC with CV are in most cases larger than MC without. We suspect that it is because the Feller condition does not satisfy. Hence, we make the vol of vol parameters four times smaller (all the parameters are kept unchanged)

L	H	K	Num of MC paths	price	relative error
1	1.6	1.2	10000	0.113813	0.18%
			400000	0.113758	0.13%
			analytical	0.113614	
1	1.5	1.2	10000	0.0769338	-0.69%
			400000	0.0775061	0.05%
			analytical	0.0774649	
1	1.4	1.2	10000	0.0376636	-0.46%
			400000	0.0378453	0.02%
			analytical	0.0378376	

Table 27: The MC price and analytic price of 1y European barrier call options in TS Heston model. The vol of vol parameters are reduced by half. The fraction of negative volatility in the simulation paths is 0.049603.

and price the same options again. Now the Feller condition satisfies. From Table 34, we can see that there is indeed faster convergence in the simulation results.

Finally we compare the prices given by ordinary Heston model and TS Heston model. From Table 35 to 37, we can see that when the barrier level is close to the current FX spot, the differences between the prices given by two models become quite large for all the options. Hence, we think that the prices of the barrier options with high chances of knock out are affected most by the model we choose.

L	H	K	MC paths	without CV	rel. error	with CV	rel. error
1	1.6	1.2	5000	0.106641	1.24%	0.105571	0.22%
			10000	0.106396	1.01%	0.105474	0.13%
			50000	0.105405	0.06%	0.105136	-0.19%
			400000	0.105337		0.105230	-0.10%
1	1.5	1.2	5000	0.0639071	-0.03%	0.0636669	-0.41%
			10000	0.0657609	2.87%	0.0648543	1.45%
			50000	0.063829	-0.15%	0.0638788	-0.07%
			400000	0.0639262		0.0639250	0.00%
1	1.4	1.2	5000	0.0164407	1.93%	0.0161899	0.38%
			10000	0.0166759	3.39%	0.0164255	1.84%
			50000	0.0161817	0.33%	0.0162892	0.99%
			400000	0.016129		0.0161839	0.34%
1.2	1.6	1.2	5000	0.0979302	1.88%	0.0968950	0.81%
			10000	0.0971613	1.08%	0.0962780	0.16%
			50000	0.0961731	0.06%	0.0959152	-0.21%
			400000	0.0961194		0.0960170	-0.11%
1.2	1.5	1.2	5000	0.0570276	0.19%	0.0568009	-0.21%
			10000	0.0587693	3.25%	0.0579158	1.75%
			50000	0.0569117	-0.02%	0.0569584	0.07%
			400000	0.0569211		0.0569199	0.00%
1.2	1.4	1.2	5000	0.0132047	2.32%	0.0129909	0.66%
			10000	0.0135648	5.11%	0.0133480	3.43%
			50000	0.0130648	1.24%	0.0131570	1.95%
			400000	0.0129053		0.0129520	0.36%

Table 28: The MC simulation with and without control variates (European barrier with the same maturity) for discrete (double) barrier call options with 24 barrier dates (two per month) and 1-year maturity in (ordinary) Heston model. The spot FX is 1.3621. The MC simulation results of 400000 paths without CV are used as reference values.

L	H	K	MC paths	without CV	rel. error	with CV	rel. error
1	1.6	1.2	5000	0.105665	1.86%	0.105062	1.28%
			10000	0.104448	0.69%	0.104785	1.01%
			50000	0.103923	0.18%	0.104573	0.81%
			400000	0.103734		0.104415	0.66%
1	1.5	1.2	5000	0.0632405	2.12%	0.0635905	2.68%
			10000	0.0627991	1.40%	0.0635751	2.66%
			50000	0.0618218	-0.17%	0.0627669	1.35%
			400000	0.0619301		0.0627863	1.38%
1	1.4	1.2	5000	0.0155787	0.70%	0.0158266	2.30%
			10000	0.0153124	-1.02%	0.0154863	0.10%
			50000	0.0154169	-0.35%	0.0157376	1.73%
			400000	0.0154704		0.0157514	1.82%
1.2	1.6	1.2	5000	0.0963627	2.13%	0.0957875	-0.35%
			10000	0.0951182	0.81%	0.0954397	-0.71%
			50000	0.0943931	0.04%	0.0950109	-1.15%
			400000	0.0943552		0.0950047	-1.16%
1.2	1.5	1.2	5000	0.0561794	0.12%	0.0565063	0.70%
			10000	0.0556682	-0.79%	0.0563917	0.50%
			50000	0.0547575	-2.41%	0.0556381	-0.84%
			400000	0.0561119		0.0561459	0.06%
1.2	1.4	1.2	5000	0.0125195	2.22%	0.0127315	3.95%
			10000	0.0122073	-0.33%	0.0123557	0.88%
			50000	0.0122141	-0.28%	0.0124839	1.93%
			400000	0.0122479		0.0124837	1.93%

Table 29: The MC simulation with and without control variates (European barrier with the same maturity) for discrete (double) barrier call options with 24 barrier dates (two per month) and 1-year maturity in TS Heston model. The spot FX is 1.3621. The MC simulation results of 400000 paths without CV are used as reference values.

L	H	K	MC paths	without CV	rel. error	with CV	rel. error
1	1.6	1.2	5000	0.0495362	-1.09%	0.0487641	-2.63%
			10000	0.050714	1.26%	0.0493721	-1.42%
			50000	0.0501668	0.17%	0.0499923	-0.18%
			400000	0.0500829		0.0498942	-0.38%
1	1.5	1.2	5000	0.0262222	0.87%	0.0256599	-1.29%
			10000	0.0261654	0.65%	0.0257096	-1.10%
			50000	0.02594	-0.21%	0.0260340	0.15%
			400000	0.0259953		0.0259306	-0.25%
1	1.4	1.2	5000	0.00807969	2.13%	0.00791230	0.01%
			10000	0.00784631	-0.82%	0.00771493	-2.48%
			50000	0.00773448	-2.23%	0.00779431	-1.48%
			400000	0.00791123		0.00796900	0.73%
1.2	1.6	1.2	5000	0.0401638	-2.11%	0.0394994	-3.73%
			10000	0.0413728	0.84%	0.0402249	-1.96%
			50000	0.0412637	0.57%	0.0411132	0.21%
			400000	0.0410288		0.0408665	-0.40%
1.2	1.5	1.2	5000	0.0192344	-1.34%	0.0187987	-3.58%
			10000	0.0195614	0.34%	0.0192043	-1.49%
			50000	0.0195914	0.49%	0.0196663	0.87%
			400000	0.0194957		0.0194445	-0.26%
1.2	1.4	1.2	5000	0.00469243	3.32%	0.00458750	1.01%
			10000	0.00466201	2.65%	0.00457865	0.82%
			50000	0.00451928	-0.49%	0.00455673	0.34%
			400000	0.0045415		0.00457666	0.77%

Table 30: The MC simulation with and without control variates (European barrier with the same maturity) for discrete (double) barrier call options with 5 barrier dates (one per year) and 5-year maturity in (ordinary) Heston model. The spot FX is 1.3621. The MC simulation results of 400000 paths without CV are used as reference values.

L	H	K	MC paths	without CV	rel. error	with CV	rel. error
1	1.6	1.2	5000	0.0508058	2.54%	0.0503171	1.56%
			10000	0.0501294	1.18%	0.0498881	0.69%
			50000	0.0496772	0.27%	0.0498101	0.53%
			400000	0.0495458		0.0495739	0.06%
1	1.5	1.2	5000	0.0272326	4.75%	0.0267253	2.80%
			10000	0.026663	2.56%	0.0264979	1.93%
			50000	0.0261965	0.77%	0.0262036	0.80%
			400000	0.0259966		0.0260614	0.25%
1	1.4	1.2	5000	0.00886097	2.34%	0.00855420	-1.21%
			10000	0.00876139	1.19%	0.00868838	0.34%
			50000	0.00871627	0.67%	0.00867524	0.19%
			400000	0.00865865		0.00869507	0.42%
1.2	1.6	1.2	5000	0.0420043	2.56%	0.0415758	1.52%
			10000	0.0417685	1.99%	0.0415550	1.47%
			50000	0.0409316	-0.06%	0.0410471	0.23%
			400000	0.0409543		0.0409788	0.06%
1.2	1.5	1.2	5000	0.0205757	4.85%	0.0201637	2.75%
			10000	0.0201713	2.79%	0.0200381	2.11%
			50000	0.0197968	0.88%	0.0198025	0.91%
			400000	0.0196239		0.0196757	0.26%
1.2	1.4	1.2	5000	0.00497627	-3.26%	0.00479519	-6.78%
			10000	0.00502489	-2.32%	0.00498050	-3.18%
			50000	0.00511766	-0.51%	0.00509186	-1.01%
			400000	0.00514401		0.00516708	0.45%

Table 31: The MC simulation with and without control variates (European barrier with the same maturity) for discrete (double) barrier call options with 5 barrier dates (one per year) and 5-year maturity in TS Heston model. The spot FX is 1.3621. The MC simulation results of 400000 paths without CV are used as reference values.

L	H	K	MC paths	without CV	rel. error	with CV	rel. error
1	1.6	1.2	5000	0.0407734	-1.98%	0.0422148	1.49%
			10000	0.0406413	-2.30%	0.0411847	-0.99%
			50000	0.0413646	-0.56%	0.0415505	-0.11%
			400000	0.0415962		0.0415548	-0.10%
1	1.5	1.2	5000	0.0187076	-3.90%	0.0190214	-2.29%
			10000	0.0190495	-2.15%	0.0192206	-1.27%
			50000	0.0194031	-0.33%	0.0193750	-0.47%
			400000	0.0194673		0.0194665	0.00%
1	1.4	1.2	5000	0.00451968	4.23%	0.00462109	6.57%
			10000	0.00440236	1.53%	0.00443878	2.37%
			50000	0.00434726	0.26%	0.00439316	1.31%
			400000	0.00433617		0.00434857	0.29%
1.2	1.6	1.2	5000	0.0294348	0.69%	0.0305553	4.52%
			10000	0.0283607	-2.98%	0.0287713	-1.58%
			50000	0.0288158	-1.43%	0.0289559	-0.95%
			400000	0.0292326		0.0292011	-0.11%
1.2	1.5	1.2	5000	0.011737	0.43%	0.0119559	2.30%
			10000	0.0113346	-3.01%	0.0114458	-2.06%
			50000	0.0115606	-1.08%	0.0115424	-1.24%
			400000	0.0116867		0.0116862	0.00%
1.2	1.4	1.2	5000	0.00183487	12.96%	0.00188279	15.91%
			10000	0.00164877	1.50%	0.00166417	2.45%
			50000	0.0016626	2.35%	0.00168222	3.56%
			400000	0.00162441		0.00162953	0.32%

Table 32: The MC simulation with and without control variates (European barrier with the same maturity) for discrete (double) barrier call options with 20 barrier dates (one per 3 months) and 5-year maturity in (ordinary) Heston model. The spot FX is 1.3621. The MC simulation results of 400000 paths without CV are used as reference values.

L	H	K	MC paths	without CV	rel. error	with CV	rel. error
1	1.6	1.2	5000	0.0444891	6.55%	0.0442213	5.90%
			10000	0.0424458	1.65%	0.0427088	2.28%
			50000	0.0423423	1.40%	0.0420757	0.77%
			400000	0.0417557		0.0417996	0.11%
1	1.5	1.2	5000	0.0207519	6.65%	0.0205349	5.54%
			10000	0.0198746	2.15%	0.0198993	2.27%
			50000	0.0198597	2.07%	0.0197690	1.60%
			400000	0.0194571		0.0194931	0.19%
1	1.4	1.2	5000	0.00474856	0.26%	0.00469946	-0.78%
			10000	0.00476566	0.62%	0.00471598	-0.43%
			50000	0.00477863	0.89%	0.00474737	0.23%
			400000	0.004736431		0.00473308	-0.07%
1.2	1.6	1.2	5000	0.0314424	7.14%	0.0312382	6.45%
			10000	0.0299109	1.92%	0.0301130	2.61%
			50000	0.0297154	1.26%	0.0295125	0.57%
			400000	0.029346427		0.0293131	-0.11%
1.2	1.5	1.2	5000	0.0122826	6.21%	0.0121431	5.00%
			10000	0.0114528	-0.96%	0.0114683	-0.83%
			50000	0.0117791	1.86%	0.0117205	1.35%
			400000	0.0115643		0.0115877	0.20%
1.2	1.4	1.2	5000	0.00153865	-10.17%	0.00152179	-11.15%
			10000	0.00159058	-7.14%	0.00157292	-8.17%
			50000	0.00163905	-4.31%	0.00162743	-4.99%
			400000	0.00171282		0.00171416	0.08%

Table 33: The MC simulation with and without control variates (European barrier with the same maturity) for discrete (double) barrier call options with 20 barrier dates (one per 3 months) and 5-year maturity in TS Heston model. The spot FX is 1.3621. The MC simulation results of 400000 paths without CV are used as reference values.

L	H	K	MC paths	without CV	rel. difference	MC with CV	rel. difference
1	1.6	1.2	50000	0.086303	0.86%	0.085937	0.44%
			400000	0.085563		0.085439	-0.14%
1	1.5	1.2	50000	0.042075	0.81%	0.041831	0.22%
			400000	0.041737		0.041611	-0.30%
1	1.4	1.2	50000	0.008311	-2.39%	0.008387	-1.50%
			400000	0.008515		0.008531	0.20%
1.2	1.6	1.2	50000	0.073425	0.77%	0.073084	0.31%
			400000	0.072862		0.072746	-0.16%
1.2	1.5	1.2	50000	0.031444	0.76%	0.031243	0.12%
			400000	0.031206		0.031101	-0.34%
1.2	1.4	1.2	50000	0.000932	-4.42%	0.000943	-3.29%
			400000	0.000975		0.000983	0.78%

Table 34: The MC simulation with and without control variates (European barrier with the same maturity) for discrete (double) barrier call options with 24 barrier dates (two per month) and 1-year maturity in (ordinary) Heston model. The vol of vol parameters reduced by four times. The spot FX is 1.3621. The MC simulation results of 400000 paths without CV are used as reference values.

L	H	K	MC paths	without CV	with CV	rel. difference
1	1.6	1.2	ordinary	0.105337	0.105230	-0.10%
			TS	0.103734	0.104415	0.66%
			rel. difference	1.55%	0.78%	
1	1.5	1.2	ordinary	0.0639262	0.0639250	0.00%
			TS	0.0619301	0.0627863	1.38%
			rel. difference	3.22%	1.81%	
1	1.4	1.2	ordinary	0.016129	0.0161839	0.34%
			TS	0.0154704	0.0157514	1.82%
			rel. difference	4.26%	2.75%	
1.2	1.6	1.2	ordinary	0.0961194	0.0960170	-0.11%
			TS	0.0943552	0.0950047	-1.16%
			rel. difference	1.87%	1.07%	
1.2	1.5	1.2	ordinary	0.0569211	0.0569199	0.00%
			TS	0.0561119	0.0561459	0.06%
			rel. difference	1.44%	1.38%	
1.2	1.4	1.2	ordinary	0.0129053	0.0129520	0.36%
			TS	0.0122479	0.0124837	1.93%
			rel. difference	5.37%	3.75%	

Table 35: Comparison between prices of discrete (double) barrier call options with 24 barrier dates (two per month) and 1-year maturity given by ordinary Heston model and TS Heston model using MC simulation with 400000 paths. The MC simulation results with and without control variates are shown. The spot FX is 1.3621.

L	H	K	MC paths	without CV	with CV	rel. difference
1	1.6	1.2	ordinary	0.0500829	0.0498942	-0.38%
			TS	0.0495458	0.0495739	0.06%
			rel. difference	1.08%	0.65%	
1	1.5	1.2	ordinary	0.0259953	0.0259306	-0.25%
			TS	0.0259966	0.0260614	0.25%
			rel. difference	-0.01%	-0.50%	
1	1.4	1.2	ordinary	0.00791123	0.00796900	0.73%
			TS	0.00865865	0.00869507	0.42%
			rel. difference	-8.63%	-8.35%	
1.2	1.6	1.2	ordinary	0.0410288	0.0408665	-0.40%
			TS	0.0409543	0.0409788	0.06%
			rel. difference	0.18%	-0.27%	
1.2	1.5	1.2	ordinary	0.0194957	0.0194445	-0.26%
			TS	0.0196239	0.0196757	0.26%
			rel. difference	-0.65%	-1.18%	
1.2	1.4	1.2	ordinary	0.0045415	0.00457666	0.77%
			TS	0.00514401	0.00516708	0.45%
			rel. difference	-11.71%	-11.43%	

Table 36: Comparison between prices of discrete (double) barrier call options with 5 barrier dates (one per year) and 5-year maturity given by (ordinary) Heston model and TS Heston model using MC simulation with 400000 paths. The MC simulation results with and without control variates are shown. The spot FX is 1.3621.

L	H	K	MC paths	without CV	with CV	rel. difference
1	1.6	1.2	ordinary	0.0415962	0.0415548	-0.10%
			TS	0.0417557	0.0417996	0.11%
			rel. difference	-0.38%	-0.59%	
1	1.5	1.2	ordinary	0.0194673	0.0194665	0.00%
			TS	0.0194571	0.0194931	0.19%
			rel. difference	0.05%	-0.14%	
1	1.4	1.2	ordinary	0.00433617	0.00434857	0.29%
			TS	0.004736431	0.00473308	-0.07%
			rel. difference	-8.45%	-8.12%	
1.2	1.6	1.2	ordinary	0.0292326	0.029201112	-0.11%
			TS	0.029346427	0.0293131	-0.11%
			rel. difference	-0.39%	-0.38%	
1.2	1.5	1.2	ordinary	0.0116867	0.0116862	0.00%
			TS	0.0115643	0.0115877	0.20%
			rel. difference	1.06%	0.85%	
1.2	1.4	1.2	ordinary	0.00162441	0.00162953	0.32%
			TS	0.00171282	0.00171416	0.08%
			rel. difference	-5.16%	-4.94%	

Table 37: Comparison between prices of discrete (double) barrier call options with 20 barrier dates (one per 3 months) and 5-year maturity given by (ordinary) Heston model and TS Heston model using MC simulation with 400000 paths. The MC simulation results with and without control variates are shown. The spot FX is 1.3621.

9 Future research direction: applying COS method on discrete barrier options

In Section 8, we use Monte Carlo simulation with control variates to price discrete barrier options. However, the slow error convergence in the Monte Carlo simulation is not a very satisfactory result to us. Hence, we try to develop some analytic formula to price discrete barrier options in Heston model which involves the COS method.[1]

9.1 COS expansion for option pricing in Heston model

Recall from Section 3 the transformed Heston model:

$$\begin{aligned} x &= (\mu - \frac{1}{2}v)\mathrm{d}t + \sqrt{v}\mathrm{d}W_1, \\ \mathrm{d}v &= \kappa(\theta - v)\mathrm{d}t + \sigma\sqrt{v}\mathrm{d}W_2, \\ \mathrm{Cov}[\mathrm{d}W_1, \mathrm{d}W_2] &= \rho\,\mathrm{d}t \end{aligned} \tag{129}$$

Then the continuous price of an option at time 0 if we know its value function at time T, $V(y, v_T)$, satisfies

$$\begin{aligned} e^{r\Delta t}C(x, v_0) &= \int_c^d \int_a^b V(y, v_T)p(y, v_T|x, v_0)dydv_T \\ &= \int_c^d \int_a^b V(y, v_T)p_y(y|v_T, v_0, x)p_v(v_T|v_0)dydv_T \end{aligned} \tag{130}$$

where $p(y, v_T|x, v_0)$ is the two-dimensional probability density function of log-asset price y and volatility v_T conditioned on their initial values x and v_0, $p_y(y|v_T, v_0, x)$ is the probability density function of y conditioned on v_T, v_0 and x, $p_v(v_T|v_0)$ is the probability density function of v_T conditioned on v_0, and $V(y, v_T)$ is the payoff/value of the option at T.

Feller has shown that the density of v_T conditioned on v_0 reads

$$\begin{aligned} p_v(v_T|v_0) &= ce^{-b-\hat{x}}\left(\frac{x}{b}\right)^{\frac{\alpha-1}{2}} I_{\alpha-1}(2\sqrt{b\hat{x}}) \\ &= ce^{-c(v_0e^{-\kappa T}+v_T)}\left(\frac{v_T}{v_0e^{-\kappa T}}\right)^{\frac{\alpha-1}{2}} I_{\alpha-1}(2\sqrt{b\hat{x}}) \end{aligned} \tag{131}$$

where $c = 2\kappa/[(1-e^{-\kappa T})\sigma^2]$, $b = cv_0e^{-\kappa T}$, $\hat{x} = cv_T$, $\alpha = 2\kappa\theta/\sigma^2$, and $I_\alpha(x)$ is the modified Bessel function of the first kind.

Applying trapezoidal rules on the volatility dimension to equation (130), we have

$$e^{r\Delta t}C(x, v_0) \approx \sum_{q=0}^{J_{vol}-1} p_v(u_q|v_0)w_q \int_a^b V(y, u_q)p_y(y-x|u_q, v_0)dy \tag{132}$$

[1] This part of work is mainly done in corporation with Fang Fang in 2008.

where J_{vol} is the number of points in the volatility dimension, $w_0 = w_{J_{vol}-1} = \frac{1}{2}\Delta v$ and $w_q = \Delta v$, $q = 1, 2, ..., J_{vol} - 2$, with $\Delta v = (d-c)/(J_{vol}-1)$.

Using the COS expansion for $p_y(y - x|u_q, v_0)$, we have the cosine series coefficients:

$$\begin{aligned}
&\frac{2}{b-a}\int_a^b p_y(y-x|u_q,v_0)\cos(k\pi\frac{y-a}{b-a})dy \\
=&\frac{2}{b-a}Re\left\{\int_a^b p_y(y-x|u_q,v_0)e^{ik\pi\frac{y-x}{b-a}}dy\cdot e^{ik\pi\frac{x-a}{b-a}}\right\} \\
=&\frac{2}{b-a}Re\left\{\widehat{p}(\frac{k\pi}{b-a};u_q,v_0)e^{i\frac{k\pi}{b-a}(x-a)}\right\}
\end{aligned} \tag{133}$$

where

$$\begin{aligned}
\widehat{p}(\frac{k\pi}{b-a};u_q,v_0) &= \int_a^b p_y(y-x|u_q,v_0)e^{ik\pi\frac{y-x}{b-a}}dy \\
&= \int_{a-x}^{b-x} p_y(y'|u_q,v_0)e^{i\frac{k\pi}{b-a}y'}dy' \\
&\approx \int_{-\infty}^{\infty} p_y(y'|u_q,v_0)e^{i\omega y'}dy'\Big|_{\omega=\frac{k\pi}{b-a}} \\
&= \mathbb{E}[e^{i\omega y'}]\Big|_{\omega=\frac{k\pi}{b-a}}
\end{aligned} \tag{134}$$

Remember that the truncation range $[a, b]$ is given in equation (42) and thus

$$[a-x, b-x] = \left[c_1 - L\sqrt{|c_2|},\ c_1 + L\sqrt{|c_2|}\right] \text{ with } L = 12 \tag{135}$$

which is chosen such that the truncated integral approximates the infinite counterpart very well.

The equation (134) is the conditional characteristic function of the logarithm of the stock given v_0 and v_T and is known analytically:

$$\widehat{p}(\omega; v_T, v_0) = e^{i\omega T(\mu - \frac{\kappa\rho}{\sigma}\theta)} \cdot e^{i\omega\frac{\rho}{\sigma}(v_T - v_0)} \cdot \Phi(g(\omega)) \tag{136}$$

where

$$g(\omega) = \omega\left(\frac{\kappa\rho}{\sigma} - \frac{1}{2}\right) + \frac{1}{2}i\omega^2(1-\rho^2) \tag{137}$$

and $\Phi(a)$ is the characteristic function of $\int_{t_0}^T v(s)ds$ given v_0 and v_T and is also known in closed-form:

$$\Phi(a) = c_1(a) \cdot e^{v_0 + v_T} \cdot e^{c_2(a)} \cdot \frac{I_{\alpha-1}(\sqrt{v_0 v_T}c_3(a))}{I_{\alpha-1}(2\sqrt{bx})} \tag{138}$$

where

$$
\begin{aligned}
c_1(a) &= \frac{\gamma(a)e^{-\frac{1}{2}(\gamma(a)-\kappa)T}(1-e^{-\kappa T})}{\kappa(1-e^{-\gamma(a)T})} = e^{\frac{1}{2}\kappa T}\cdot\frac{1-e^{-\kappa T}}{\kappa}\cdot\frac{\gamma(a)e^{-\frac{1}{2}\gamma(a)T}}{1-e^{-\gamma(a)T}} \\
c_2(a) &= \frac{1}{\sigma^2}\left[\frac{\kappa(1+e^{-\kappa T})}{1-e^{-\kappa T}} - \frac{\gamma(a)(1+e^{-\gamma(a)T})}{1-e^{-\gamma(a)T}}\right] \\
c_3(a) &= \frac{4}{\sigma^2}\frac{\gamma(a)e^{-\frac{1}{2}\gamma(a)T}}{1-e^{-\gamma(a)T}} \\
\gamma(a) &= \sqrt{\kappa^2 - 2\sigma^2 ai}
\end{aligned}
\tag{139}
$$

Hence, we can expand $p_y(y-x|u_q,v_0)$ in its cosine series:

$$
p_y(y-x|u_q,v_0) \approx \frac{2}{b-a}\sum_{k=0}^{N-1}{}'Re\left\{\widehat{p}(\frac{k\pi}{b-a};u_q,v_0)e^{i\frac{k\pi}{b-a}(x-a)}\right\}\cos(k\pi\frac{y-a}{b-a}) \tag{140}
$$

Substitute (140) into (132), we get

$$
\begin{aligned}
e^{r\Delta t}C(x,v_0) \approx & \sum_{q=0}^{J_{vol}-1} p_v(u_q|v_0)w_q \\
& \frac{2}{b-a}\sum_{k=0}^{N-1}{}'\int_a^b V(y,u_q)Re\left\{\widehat{p}(\frac{k\pi}{b-a};u_q,v_0)e^{i\frac{k\pi}{b-a}(x-a)}\right\}\cos(k\pi\frac{y-a}{b-a})dy \\
\approx & \sum_{q=0}^{J_{vol}-1} p_v(u_q|v_0)w_q\frac{2}{b-a}\sum_{k=0}^{N-1}{}'\int_a^b V(y,u_q)\cos(k\pi\frac{y-a}{b-a})dy \\
& \cdot Re\left\{\widehat{p}(\frac{k\pi}{b-a};u_q,v_0)e^{i\frac{k\pi}{b-a}(x-a)}\right\}
\end{aligned}
\tag{141}
$$

Set $\widehat{V}_{k,q} := \frac{2}{b-a}\int_a^b V(y,u_q)\cos(k\pi\frac{y-a}{b-a})dy$, thus

$$
e^{r\Delta t}C(x,v_0) \approx \sum_{q=0}^{J_{vol}-1} p_v(u_q|v_0)w_q\sum_{k=0}^{N-1}{}'\widehat{V}_{k,q}Re\{\widehat{p}(\frac{k\pi}{b-a};u_q,v_0)e^{i\frac{k\pi}{b-a}(x-a)}\} \tag{142}
$$

Define $\phi(\frac{k\pi}{b-a};u_q,v_0) = p_v(u_q|v_0)\widehat{p}(\frac{k\pi}{b-a};u_q,v_0)$, then

$$
\begin{aligned}
e^{r\Delta t}C(x,v_0) &\approx \sum_{q=0}^{J_{vol}-1}\sum_{k=0}^{N-1}{}'\widehat{V}_{k,q}Re\left\{\phi(\frac{k\pi}{b-a};u_q,v_0)e^{i\frac{k\pi}{b-a}(x-a)}\right\}w_q \\
&= \sum_{q=0}^{J_{vol}-1}\sum_{k=0}^{N-1}{}'\widehat{V}_{k,q}P_{k,q}(x,v_0)
\end{aligned}
\tag{143}
$$

where

$$P_{k,q}(x,v_0) = Re\{\phi(\frac{k\pi}{b-a};u_q,v_0)e^{i\frac{k\pi}{b-a}(x-a)}\}w_q \tag{144}$$

Note that when we multiply $p_v(u_q|v_0)$ and $\widehat{p}(\frac{k\pi}{b-a};u_q,v_0)$ to get $\phi(\frac{k\pi}{b-a};u_q,v_0)$, we find that the modified Bessel function $I_{\alpha-1}(2\sqrt{bx})$ in $p_v(u_q|v_0)$ and $\widehat{p}(\frac{k\pi}{b-a};u_q,v_0)$ cancel each other out. Hence, the expression for $\phi(\frac{k\pi}{b-a};u_q,v_0)$ can be simplified:

$$\begin{aligned}\phi(\frac{k\pi}{b-a};u_q,v_0) =& p_v(u_q|v_0)\cdot\widehat{p}(\frac{k\pi}{b-a};u_q,v_0) &(145)\\ =& ce^{-c(v_0e^{-\kappa T}+v_T)}\left(\frac{v_T}{v_0e^{-\kappa T}}\right)^{\frac{\alpha-1}{2}}\\ & \cdot e^{i\omega T(r-\frac{\kappa\rho}{\sigma}\theta)}\cdot e^{i\omega\frac{\rho}{\sigma}(v_T-v_0)}\cdot c_1(g(\omega))\cdot e^{v_0+v_T}\cdot e^{c_2(g(\omega))}\\ & \cdot I_{\alpha-1}\sqrt{v_0v_T}\cdot c_3(a) &(146)\\ =& f(\omega)\cdot e^{Av_0}v_0^{\frac{1-\alpha}{2}}\cdot e^{Bv_T}v_T^{\frac{\alpha-1}{2}}\cdot I_{\alpha-1}\sqrt{v_0v_T}\cdot c_3(a) &(147)\end{aligned}$$

where

$$\begin{cases} f(\omega) &= ce^{\kappa T\frac{\alpha-1}{2}}e^{i\omega T(r-\frac{\kappa\rho}{\sigma}\theta)}c_1(g(\omega))e^{c_2(g(\omega))}\\ k(\omega) &= c_3(\omega)\\ A &= -ce^{-\kappa T}-i\omega\frac{\rho}{\sigma}+c_2(g(\omega))\\ B &= -c+i\omega\frac{\rho}{\sigma}+c_2(g(\omega))\end{cases}$$

9.2 Recursion formula for discrete barrier option

For discretely monitored "out" barrier options, suppose we have two barrier levels, L and H, with $L < S_0 < H$. Define $h_{up} = ln(H)$ and $h_{down} = ln(L)$.

The payoff function for a discrete barrier option at maturity reads

$$\begin{aligned}V(x,T) &= \{max(\alpha(S_T-K),0)-Rb\}\,\mathbf{1}_{\{L<S_{t_i}<H\}}+Rb\\ &= \left\{[\alpha K(e^x-1)]^+-Rb\right\}\mathbf{1}_{\{h_{down}<x_{t_i}<h_{up}\}}+Rb\end{aligned} \tag{148}$$

where $\alpha = 1$ for a call and $\alpha = -1$ for a put, $x = log(S_T/K)$, $x_{t_i} = log(S_{t_i}/K)$ and Rb is a rebate.

At barrier date t_m before maturity, if the spot has not breached the barrier, $V(y,u_q,t_m)$ is equal to its continuous value given in equation (143):

$$C(x,v_0,t_m) = e^{-r\Delta t}\sum_{q=0}^{J_{vol}-1}{}'\sum_{k=0}^{N-1}{}'P_{k,q}(x,v_0)\widehat{V}_{k,q}(t_{m+1}) \tag{149}$$

According to the definition of $\widehat{V}_{k,q}(t_m)$, we have

$$\begin{aligned}
\widehat{V}_{k,q}(t_m) &= \frac{2}{b-a}\int_a^b V(y,u_q,t_m)\cos(k\pi\frac{y-a}{b-a})dy \\
&= \frac{2}{b-a}\int_{x_1}^{x_2} C(y,u_q,t_m)\cos(k\pi\frac{y-a}{b-a})dy \\
&\quad +\frac{2}{b-a}\int_a^{x_3} e^{-r(T-t_m)}Rb\cos(k\pi\frac{y-a}{b-a})dy \\
&\quad +\frac{2}{b-a}\int_{x_4}^{b} e^{-r(T-t_m)}Rb\cos(k\pi\frac{y-a}{b-a})dy \\
&:= \widehat{c}_{k,q}(x_1,x_2,t_m) + e^{-r(T-t_m)}Rb\frac{2}{b-a}[\psi_k(a,x_3)+\psi_k(x_4,b)] \qquad (150)
\end{aligned}$$

where equation (124) is applied. $x_1 = \max\{a, h_{down}, 0\}$, $x_2 = \min\{b, h_{up}\}$ for a call, and $x_1 = \max\{a, h_{down}\}$, $x_2 = \min\{b, h_{up}, 0\}$ for a put. For both call and put, $x_3 = \max\{a, h_{down}\}$ and $x_4 = \min\{b, h_{up}\}$. Clearly, $a \le x_3 \le x_1 \le x_2 \le x_4 \le b$.

Thus, substitute (149) into the definition of $\widehat{c}_{k,q}(x_1,x_2,t_m)$, we have

$$\begin{aligned}
\widehat{c}_{k,q}(x_1,x_2,t_m) &= \frac{2}{b-a}\int_{x_1}^{x_2} C(y,u_q,t_m)\cos(k\pi\frac{y-a}{b-a})dy \\
&= \frac{2}{b-a}e^{-r\Delta t}\sum_{n=0}^{J_{vol}-1}{\sum_{l=0}^{N-1}}'\int_{x_1}^{x_2} P_{l,n}(y,u_q)\cos(k\pi\frac{y-a}{b-a})dy\cdot\widehat{V}_{l,n}(t_{m+1})
\end{aligned} \qquad (151)$$

Substitute the definition of $P_{l,n}$ in (144) into the above equation, we have

$$\begin{aligned}
\widehat{c}_{k,q}(x_1,x_2,t_m) &= \frac{2}{b-a}e^{-r\Delta t}\sum_{n=0}^{J_{vol}-1}{\sum_{l=0}^{N-1}}'\widehat{V}_{l,n}(t_{m+1}) \\
&\quad \cdot\int_{x_1}^{x_2} Re\{\phi(\frac{l\pi}{b-a};u_n,v_0)e^{i\frac{l\pi}{b-a}(y-a)}\}w_n\cos(k\pi\frac{y-a}{b-a})dy \\
&= e^{-r\Delta t}Re\{{\sum_{l=0}^{N-1}}'\{\sum_{n=0}^{J_{vol}-1}\widehat{V}_{l,n}(t_{m+1})\phi(\frac{l\pi}{b-a};z_n,u_q)w_n\}M_{k,l}(x_1,x_2)\} \qquad (152)
\end{aligned}$$

where $M_{k,l}(x_1,x_2) = \frac{2}{b-a}\int_{x_1}^{x_2} e^{i\frac{l\pi}{b-a}(y-a)}\cos(k\pi\frac{y-a}{b-a})dy$.

At the maturity ($t_m = T$), we have

$$\begin{aligned}\widehat{c}_{k,q}(x_1,x_2,T) &= \frac{2}{b-a}\int_{x_1}^{x_2} C(y,u_q,T)\cos(k\pi\frac{y-a}{b-a})dy \\ &= \frac{2}{b-a}\int_{x_1}^{x_2} V(y,T)\cos(k\pi\frac{y-a}{b-a})dy \\ &= \frac{2}{b-a}\int_{x_1}^{x_2} \alpha K(e^y-1)\cos(k\pi\frac{y-a}{b-a})dy \\ &= \frac{2}{b-a}\alpha K\left[\chi_k(x_1,x_2)-\psi_k(x_1,x_2)\right] \end{aligned} \tag{153}$$

and substitute it into (150),

$$\widehat{V}_{k,q}(T) = \frac{2}{b-a}\alpha K\left[\chi_k(x_1,x_2)-\psi_k(x_1,x_2)\right] + \frac{2}{b-a}Rb[\psi_k(a,x_3)+\psi_k(x_4,b)] \tag{154}$$

which is actually independent of q, the volatility dimension.

Hence, starting from $\widehat{V}_{k,q}(T)$, we can recursively get the coefficients $\widehat{V}_{k,q}(t_m)$ for all the previous barrier dates t_m and finally the option value $c(x,v_0,t_0)$ at the pricing date.

9.3 Problems now in pricing discrete barrier option using COS method

Despite that we can show quite nice formula for pricing the discrete barrier options using the COS method, we find that we get quite large errors when we implement the algorithm and do the pricing, especially when the Feller condition does not satisfy. Hence, we still need to dive into the algorithm and try to improve it. This will be our task in the future.

10 Conclusion

The original Heston model contains constant parameters. In order to incorporate the term structure of the implied volatility surface, we allow for time-dependent parameters. We choose the time-dependence to be piecewise constant and show how in this case the model can be calibrated in an efficient way. A key ingredient is the characteristic function, where we show the derivation of its analytic formula in the TS Heston model in Section 3. We then apply the COS pricing method on it to price European-style options in Section 4. Since the COS method provides us with a semi-analytic solution for pricing European-style options, we can price them fast and accurately. In Section 5, we choose 3 parameters in the Heston model to be time-dependent, the correlation, vol of vol and mean reversion level. These three will be included in the calibration. The mean reversion rate is not included in the calibration, it is treated as an unobservable parameter not determined by the market in our approach. We consider the initial guess of the parameters used in the calibration, as well as an analytical estimate for a minimum value of the mean reversion rate in the deterministic case. We test the calibration on the market data for EUR/USD and USD/JPY in Section 6. For the most liquid part of these volatility surfaces, up to 5-year maturity, we show that the TS Heston model can be calibrated with high accuracy. This requires a mean reversion rate of 2 or higher for EUR/USD. Interestingly, for USD/JPY calibration requires some term structure in the mean reversion rate as well.

In order to see whether the model is sufficiently robust in the calibration of different market data, we test our TS Heston model by calibrating it to the historic data spanning a whole year in Section 7. Before that, we perform jump tests on the historic market data to find out whether jumps are present or not. We have found that there are no jumps in the EUR/USD market data, but jumps do exist in the USD/JPY market data. Hence, for the USD/JPY market, models with jumps (e.g. Bates' model) might be preferred. Since from this conclusion it seems that models without jumps might apply for the EUR/USD market data, we calibrate our model to the EUR/USD historic data spanning a whole-year period from Sep. 3, 2007 to Aug. 29, 2008. We find that most of the calibrations (61.24%) fail at the 6-year maturity and the success of the calibration indeed depends on the market data. We also find that we can only expect stable parameters over time when the market data remains stable. Changing model parameters therefore requires us to take extra effort in hedging.

After the calibration, we now try to price some exotic options using the TS Heston model we have calibrated in Section 8. In the Black-Scholes model, the analytic formula for continuous (double) barrier options exists and we can use them as control variates for the pricing of discrete (double) barrier options in the Monte Carlo simulation. In the Heston model, we are not aware of the analytic formula for these two options. Therefore, to price the discrete barrier options in the TS Heston model, we use Monte Carlo simulation with control variates. Here, we propose to use the European barrier option with the same maturity as the discrete barrier option as a new control variate. We have shown that using this alone can already greatly reduce the variance. When the maturity of the option is short and the number of

barrier dates is small, the effect of variance reduction is most significant. We have also found that sometimes there is discrepancy between the MC simulation results with control variates and those without because the MC simulation results of the control variates do not converge to their analytic values. We think it happens because the Feller condition does not satisfy. Hence, in our view, the MC simulation with CV not only reduces the variance, but helps to eliminate the biases as well. In addition, we have compared the simulation results from the Heston model and the TS Heston model as well, and have found that the prices of the barrier options with high chances of knock out are affected most by the model we choose.

Finally, we propose to apply the COS method on discrete barrier options as a future research direction in Section 9. We have derived the COS expansion formula for option pricing in the Heston model and the recursion formula for the discrete (double) barrier options. Although the current pricing results using the COS method still have quite large errors, we think that given time this algorithm can be improved and nice results will come out. Hence, this will be our research direction in the future.

References

[1] B. Nauta and V. Braude, *Project description: the Heston model with term structure, ABN AMRO internal note*, 2008.

[2] R. Beneder, *Validation of the volatility smile interpolation in MUREX, ABN AMRO internal note* , VAL03-01, 2003.

[3] F. Fang and C.W. Oosterlee, *A novel pricing method for European options based on Fourier-cosine series expansions*, SIAM Journal on Scientific Computing, 2008.

[4] A. Elices, *Models with time-dependent parameters using transform methods: application to Heston's model*. See http://arxiv.org/abs/0708.2020.

[5] R. Lord and C. Kahl, *Complex logarithms in the Heston-like models*, forthcoming in Mathematical Finance, 2009. See http://ssrn.com/abstract_id=1105998.

[6] P.P. Carr and D.B. Madan, *Option valuation using the fast Fourier transform*. J. Comp. Finance, 2:61-73, 1999.

[7] J. Hakala and U. Wystup, *Foreign Exchange Risk - Models, Instruments and Strategies*, Risk Books, 2002.

[8] S. Mikhailov and U. Nögel, *Heston Stochastic Volatility Model Implementation, Calibration and Some Extensions*, Wilmott magazine, 74, (July 2003).

[9] M. Overhaus, A. Bermudez, H. Buehler, A. Ferraris, C. Jordinson and A. Lamnouar, *Equity Hybrid Derivatives*, P.36, John Wiley & Sons, 2007.

[10] J.C. Ndogmo, *Some Control Variates for exotic options*. See http://arxiv.org/abs/0806.4675.

[11] Kevin Cheng, *An Overview of Barrier Options*. See http://www.global-derivatives.com/docs/OverviewofBarrierOptions_(Cheng)_2003.pdf.

[12] Y.K. Kwok, *Double barrier options*, Encyclopedia of Financial Engineering and Risk Management, Fitzroy Dearborn Publishers, 2006. See http://www.math.ust.hk/~maykwok/piblications/Articles/doubarencyclo.pdf.

[13] A. Li, *The Pricing of Double Barrier Options and Their Variations*, Advances in Futures and Options Research, Vol. 10, 1998. See http://ssrn.com/abstract=772046.

[14] S.G. Kou, *On Pricing Of Discrete Barrier Options*, Statistica Sinica, Vol. 13:955-964, 2003. See http://www.columbia.edu/~sk75/sinica.pdf.

[15] F. Fang and C.W. Oosterlee, *Pricing Early-Exercise and Discrete Barrier Options by Fourier-Cosine Series Expansions*. See http://ta.twi.tudelft.nl/mf/users/oosterle/oosterlee/bermCOS.pdf.

[16] S.A. Griebsch and U. Wystup, *On the Valuation of Fader and Discrete Barrier Options in Heston's Stochastic Volatility Model*, working paper. See http://papers.ssrn.com/sol3/papers.cfm?abstract_id=1310422.

[17] Global Derivatives v3.0, *Parisian Options*. See http://www.global-derivatives.com/index.php?option=com_content&task=view&id=43.

[18] C. Chu, *Applying the Control Variate Technique to Numerical Option Pricing Models*. See http://thesis.lib.ncu.edu.tw/ETD-db/ETD-search/view_etd?URN=88425010.

[19] E. Derman, I. Kani and D. Ergener, *Static Options Replication.. Journal of Derivatives*, summer: 78-95, 1995.

[20] Y. Ait-Sahalia and J. Jacod, *Testing for Jumps in a Discretely Observed Process*, Finance International Meeting AFFI, December 2007, Paris. See http://ssrn.com/abstract=1069872.

[21] Wikipedia, *Heston model*. See http://en.wikipedia.org/wiki/Heston_model.

[22] *Derivatives Week*, May 29th, 1995.

[23] P.P. Carr, H. Geman, D.B. Madan and M. Yor, *The fine structure of asset returns: An empirical investigation*. J. of Business, 75: 305-332, 2002.

[24] B. Dupire, *Pricing and hedging with smiles*, Proc. AFFI Conf., LaBaule 1993; *Pricing with a smile*, Risk magazine, **7** (1), 18 (1994).

[25] S. L. Heston, *A Closed-Form Solution for Options with Stochastic Volatility with Applications to Bond and Currency Options*, The Review of Financial Studies, **6**, 327 (1993).

[26] M. Bouev, *FX with Stochastic Volatility, ABN AMRO internal note*, 2007.

[27] J. Rizov, *Heston Model Calibration in the EFFEX-Framework*, OTH08-07.

[28] J. Gatheral, *The Volatility Surface, a Practitioner's Guide*, John Wiley & Sons, 2006.

[29] C. Kahl and P. Jäckel, *Not-So-Complex Logarithms in the Heston Model*, Wilmott Magazine, **19**, 94 (2005).

[30] T. Mexner, *The Heston Stochastic Volatility Model in Dolphin, ABN AMRO internal note*, VAL07-73, 2007.

A Appendix: market data

Tenor	volATMs	volRR25s	volBF25s	Delta type	Discount factors (EUR)	Discount factors (USD)
1d	31.000%	-1.500%	0.450%	Pips	100.00%	99.99%
1w	22.000%	-1.300%	0.450%	Pips	99.96%	99.89%
2w	21.000%	-1.300%	0.450%	Pips	99.90%	99.79%
1m	20.000%	-1.300%	0.450%	Pips	99.65%	99.54%
2m	17.864%	-1.097%	0.501%	Pips	99.24%	99.15%
3m	16.772%	-1.006%	0.523%	Pips	98.84%	98.76%
6m	15.092%	-0.902%	0.501%	Pips	97.73%	97.80%
9m	14.495%	-0.804%	0.524%	Pips	96.39%	96.74%
1y	14.200%	-0.700%	0.550%	Pips	95.26%	95.72%
2y	13.947%	-0.650%	0.550%	PipsForward	93.28%	94.46%
3y	13.600%	-0.650%	0.550%	PipsForward	89.12%	90.94%
4y	13.199%	-0.650%	0.500%	PipsForward	85.64%	87.45%
5y	12.801%	-0.650%	0.500%	PipsForward	82.03%	83.76%
6y	11.902%	-0.401%	0.375%	PipsForward	78.53%	80.01%
7y	11.401%	-0.400%	0.375%	PipsForward	75.02%	76.31%
8y	10.952%	-0.400%	0.375%	PipsForward	71.59%	72.70%
9y	10.501%	-0.400%	0.375%	PipsForward	67.97%	69.22%
10y	10.100%	-0.400%	0.375%	PipsForward	65.20%	65.89%
12y	9.353%	-0.599%	0.325%	Simple	59.46%	59.96%
15y	8.601%	-0.600%	0.325%	Simple	51.96%	52.03%
20y	8.550%	-0.600%	0.325%	Simple	42.70%	41.66%
25y	8.450%	-0.600%	0.325%	Simple	36.13%	33.60%
30y	8.450%	-0.600%	0.325%	Simple	31.00%	27.30%

Table 38: EUR/USD market data, the spot FX is 1.3621 USD/EUR

Tenor	volATMs	volRR25s	volBF25s	Delta type	Discount factors (USD)	Discount factors (JPY)
1d	20.000%	-0.750%	0.160%	Percent	100.00%	100.00%
1w	12.879%	-0.950%	0.180%	Percent	99.91%	99.99%
2w	12.374%	-1.450%	0.200%	Percent	99.81%	99.99%
1m	12.176%	-1.913%	0.241%	Percent	99.57%	99.97%
2m	11.717%	-2.288%	0.269%	Percent	99.09%	99.93%
3m	11.440%	-2.627%	0.307%	Percent	98.68%	99.90%
6m	11.116%	-3.182%	0.378%	Percent	97.40%	99.77%
9m	10.819%	-3.487%	0.428%	Percent	96.12%	99.58%
1y	10.700%	-3.800%	0.480%	Percent	94.86%	99.37%
2y	10.149%	-4.301%	0.510%	PercentForward	90.15%	98.23%
3y	9.950%	-4.801%	0.530%	PercentForward	85.82%	96.80%
4y	10.000%	-5.049%	0.580%	PercentForward	81.57%	95.08%
5y	10.050%	-5.299%	0.580%	PercentForward	77.45%	93.16%
6y	10.200%	-5.549%	0.550%	PercentForward	73.50%	91.10%
7y	10.399%	-5.650%	0.550%	PercentForward	69.70%	88.91%
8y	11.050%	-5.750%	0.550%	PercentForward	66.10%	86.67%
9y	11.750%	-5.850%	0.550%	PercentForward	62.66%	84.37%
10y	12.546%	-5.900%	0.550%	PercentForward	59.31%	82.02%
12y	13.247%	-6.099%	1.406%	Simple	53.14%	77.35%
15y	14.699%	-6.200%	1.460%	Simple	44.98%	70.60%
20y	16.747%	-6.300%	1.510%	Simple	34.09%	60.30%
25y	18.696%	-6.400%	1.560%	Simple	25.94%	51.43%
30y	19.946%	-6.400%	1.610%	Simple	19.86%	44.17%

Table 39: USD/JPY market data, the spot FX is 118.95 JPY/USD